

Representing Random Utility Choice Models with Neural Networks

Ali Aouad

London Business School, aaouad@london.edu.

Antoine Désir

INSEAD, antoine.desir@insead.edu.

Motivated by the successes of deep learning, we propose a class of neural network-based discrete choice models, called RUMnets, which is inspired by the random utility maximization (RUM) framework. This model formulates the agents' random utility function using the sample average approximation (SAA) method. We show that RUMnets sharply approximate the class of RUM discrete choice models: any model derived from random utility maximization has choice probabilities that can be approximated arbitrarily closely by a RUMnet. Reciprocally, any RUMnet is consistent with the RUM principle. We derive an upper bound on the generalization error of RUMnets fitted on choice data, and gain theoretical insights on their ability to predict choices on new, unseen data depending on critical parameters of the dataset and architecture. By leveraging open-source libraries for neural networks, we find that RUMnets outperform other state-of-the-art choice modeling and machine learning methods by a significant margin on two real-world datasets.

1. Introduction

Many businesses offer customers an assortment of products and services to choose from, whether it be a movie to watch, a restaurant to order from, or a product to buy. An important task for these organisations is therefore to predict customers' choices using historical data in order to inform tactical decisions such as assortment, pricing or matching optimization. One key challenge in these settings is the presence of substitution effects: the demand for a particular product depends on what else is offered. Discrete choice models, which describe the probability that a random customer chooses a given alternative out of any assortment of products, are used to model such substitution behaviors. Considerable scientific research in marketing, economics, and operations research has focused on various probabilistic and parametric specifications of discrete choice models.

In recent years, however, research on choice modeling has developed into a new horizon with the incorporation of machine learning (ML) and deep learning (DL) methods. Powered by advances in algorithms, computing power and availability of data, such methods are used for a vast array of tasks such as speech recognition, natural language processing and image classification. Hence, researchers have attempted to take advantage of ML/DL methods in the context of demand estimation and choice modeling. This rapidly growing literature focuses on two main considerations.

From an implementation perspective, we may leverage open source ML/DL libraries (such as automated differentiation tools) to estimate large-scale choice models, bypassing traditional barriers in terms of number of parameters and volume of data. Along these lines, one approach focuses on (overparametrized) variants of the MNL model, whose implementation is very convenient using deep learning libraries (Wang et al. 2021, Han et al. 2020). Other papers, however, have offered a more drastic approach: choice modeling can be formulated as a classification problem with multiple classes. With this view, the estimation of a choice model can be cast into training popular ML/DL classifiers, such as Random Forests or deep neural networks. However, this “model-free” logic means that the probabilistic structure of classical choice models (such as the rationality axiom or Independence of Irrelevant Alternatives property) can be lifted all-together. While training these predictive algorithms in theory may require large amounts of data, recent empirical studies have shown that this approach is successful on several real-world choice datasets (Wong and Farooq 2019, Chen et al. 2019, Chen and Mišić 2020).

Our research takes the task of developing a general, and yet structured approach to choice modeling that leverages neural networks for purposes of estimation. Our work revisits the *random utility maximization* (RUM) principle, which is the overarching framework for most parametric choice models (McFadden and Train 2000, Train 2009). Assuming that customers are rational, the RUM principle states that customers assign a utility to each product and simply choose the one with the highest utility. The firm cannot observe the customer’s utility but only has access to observable attributes of the product and customer. For this reason, the utility is assumed to be stochastic from the point of view of the firm. The randomness in the utility allows capturing unobserved heterogeneity in customers and products. Different structural and distributional assumptions on the utility function lead to different RUM discrete choice models including the multinomial logit (MNL) model (Luce 1959, McFadden 1974), the latent-class MNL (McFadden and Train 2000) or the nested logit model (Williams 1977). The validity of a RUM model heavily relies on the utility function and distributional assumption specified by the modeler.

Thinking of the RUM principle as a “minimal” structure for choice models, we ask the following questions: can the class of *all* RUM discrete choice models be efficiently approximated by a compact neural network architecture? Can the resulting neural network be trained on limited choice data? How does this approach compare to model-free methods in terms of prediction accuracy?

Preview of our results. Our main contribution is to develop a neural network architecture, RUMnet, that provides a sharp representation of RUM discrete choice models. Contrary to model-free classification methods, our approach retains the RUM principle as an underlying structure of

customers’ probabilistic choices. The core idea is to approximate the customers’ random utility using a sample average approximation (SAA). We formally establish that RUMnets tightly capture the class of all RUM discrete choice models. In particular, their choice probabilities can be approximated arbitrarily closely by those of a RUMnet architecture, and vice versa. This implies that the class of RUMnet discrete choice models is very general and subsumes as special cases the MNL model, mixture of MNLs, and related parametric models. Analytically, we derive an upper bound on the generalization errors of RUMnets fitted on choice data, i.e., the difference between their out-of-sample and in-sample log-likelihoods. Remarkably, this bound does not grow with the number of distinct samples of the SAA, while its dependence on the cardinality of the assortments is improved compared to existing results. These findings suggest that the estimation of RUMnets is well-behaved, even for certain deep architectures and large assortments. We further show that any RUMnet admits a compact SAA approximation using a relatively small number of samples.

Empirically, we demonstrate that RUMnets can be easily estimated on real-world data by leveraging widely used open-source libraries ¹. On two different datasets, RUMnets achieve a robust predictive accuracy and outperform other benchmarks by a significant margin. In contrast, the performance of model-free methods such as random forests varies across these datasets. We hypothesize that, contrary to RUMnets, their predictive performance is affected by the input dimension (i.e., number of attributes and distinct products). We conduct synthetic experiments in a controlled environment, where the ground truth is known, to support these hypotheses and validate our architecture. Overall, RUMnets may offer a practical middle ground between a general expressive power and an interpretable utility-based representation of the agents’ choice-making process.

Directed related literature. The idea of bridging ML/DL methods with choice modeling has received a great deal of attention in the recent literature. Several papers develop various neural network-based implementations of the MNL choice model (Bentz and Merunka 2000, Sifringer et al. 2020, Wang et al. 2020). In particular, Han et al. (2020) consider a special case of this architecture, called TasteNet, where customers’ attributes feed into a neural network that outputs a taste vector, which corresponds to the coefficients of the product attributes within a linear utility function. Along the same lines, Gabel and Timoshenko (2021) develops a binary logit choice model and employs neural networks to learn representations of customers’ purchase history and other observable attributes. In these logit-based models, the weights of the neural networks are shared across products, thus allowing the models to be scaled to large assortments (Wang et al. 2021).

¹ All our code is open-source and can be found at github.com/antoinedesir/RUMnet.

In contrast with the above approach, a growing number of papers employ generic ML classifiers and relax the probabilistic structure of parametric choice models altogether. For example, [Chen et al. \(2019\)](#) and [Chen and Mišić \(2020\)](#) train random forests to predict choices, while [Jiang et al. \(2020\)](#) use a graphical Lasso method. The resulting probabilistic models have the ability to capture a variety of choice behaviors including complementarities between products ([Jiang et al. 2020](#)), contextual effects ([Rosenfeld et al. 2020](#)), and even irrational behaviors ([Berbeglia 2018](#)). Many of these models amount to a class of universal approximators, which generally violates the RUM principle ([McFadden and Train 2000](#)). Despite their strong predictive power demonstrated in recent literature, these model-free methods are in theory harder to estimate from limited data, and they may not capture generalizable relationships. For example, the importance of modelling the substitution behavior realistically is highlighted by the randomized experiment of [Feldman et al. \(2018\)](#) in the context of assortment optimisation. Reflecting this challenge, our approach combines the RUM principle, as depicted by [McFadden and Train \(2000\)](#), with the expressive power of neural networks. RUMnets are also closely related to the class of rank-based choice models ([Rusmevichientong et al. 2006](#), [Farias et al. 2013](#)). A key contribution of our work, however, is to capture varying contextual attributes.

2. A Sharp Neural Network Architecture for RUM Choice Models

In this section, we introduce our neural network architecture, RUMnet, which closely imitates the RUM principle, meaning that a representative agent chooses over different alternatives by comparing their random utilities.

2.1. RUM discrete choice models

We begin by introducing some notation and the class of RUMs ([McFadden and Train 2000](#)). Each product is associated with a vector of d_x observable features, or attributes, denoted by \mathbf{x} , varying in a compact set $\mathcal{X} \subseteq \mathbb{R}^{d_x}$. Additionally, we let $\boldsymbol{\epsilon}(\mathbf{x})$ denotes a random vector of unobserved attributes of size d_ϵ , corresponding to a random experiment over $[0, 1]^{d_\epsilon}$. This random vector captures unobserved (i.e., latent) heterogeneity in the products. Here, the notation $\boldsymbol{\epsilon}(\mathbf{x})$ indicates that the distribution of the alternative’s unobserved component might depend on its observed component \mathbf{x} . Similarly, each customer is described by a vector of d_z observable attributes, denoted by \mathbf{z} , varying in a compact set $\mathcal{Z} \subseteq \mathbb{R}^{d_z}$. The customer also has a vector of d_ν unobserved (idiosyncratic) attributes $\boldsymbol{\nu}(\mathbf{z})$, which correspond to a random experiment over $[0, 1]^{d_\nu}$. We further assume that $\boldsymbol{\epsilon}(\mathbf{x})$ and $\boldsymbol{\nu}(\mathbf{z})$ are mutually independent and uniformly distributed continuous random fields. Importantly, even though $\boldsymbol{\epsilon}(\mathbf{x})$ and $\boldsymbol{\nu}(\mathbf{z})$ are independent given \mathbf{x} and \mathbf{z} , their dependence on \mathbf{x} and \mathbf{z} may capture relationships between products and individuals. Finally, we specify a utility function $U : \mathcal{X} \times [0, 1]^{d_x} \times \mathcal{Z} \times [0, 1]^{d_z} \rightarrow \mathbb{R}$ which is assumed to be bounded and uniformly continuous in its

arguments. For $\mathbf{x} \in \mathcal{X}$ and $\mathbf{z} \in \mathcal{Z}$, $U(\mathbf{x}, \boldsymbol{\epsilon}(\mathbf{x}), \mathbf{z}, \boldsymbol{\nu}(\mathbf{z}))$ quantifies how a customer with attributes \mathbf{z} values an offered product with attributes \mathbf{x} . This quantity is random due to $\boldsymbol{\epsilon}(\mathbf{x})$ and $\boldsymbol{\nu}(\mathbf{z})$.

We now describe the probabilistic outcomes for any given *choice event* (\mathbf{z}, A) , where a customer with observable attributes $\mathbf{z} \in \mathcal{Z}$ is offered a finite assortment of alternatives $A \subseteq \mathcal{X}$. Throughout the remainder of the paper, we assume A is finite and satisfies $|A| \leq \kappa$ for some integer $\kappa \geq 0$. The RUM principle implies that the customer picks the highest-utility product in the assortment A . Specifically, denoting by $\pi(\mathbf{x}, \mathbf{z}, A)$ the probability that a customer with observable attributes \mathbf{z} chooses $\mathbf{x} \in A$, we have

$$\pi(\mathbf{x}, \mathbf{z}, A) = \Pr_{\boldsymbol{\epsilon}, \boldsymbol{\nu}} [U(\mathbf{x}, \boldsymbol{\epsilon}(\mathbf{x}), \mathbf{z}, \boldsymbol{\nu}(\mathbf{z})) > U(\mathbf{x}', \boldsymbol{\epsilon}(\mathbf{x}'), \mathbf{z}, \boldsymbol{\nu}(\mathbf{z})) \text{ , } \forall \mathbf{x}' \in A \setminus \mathbf{x}] \text{ .}$$

To ensure that the distribution $\{\pi(\mathbf{x}, \mathbf{z}, A)\}_{\mathbf{x} \in A}$ is well-defined, we assume that ties between the product utilities occur with probability zero. The family of RUMs subsumes a large array of models used in practice such as the MNL model, the nested logit model, and their probabilistic mixtures.

2.2. RUMnet

In the RUM framework, the utility function is a random field. Our main idea is to approximate this random field using a sample average approximation (SAA). Each sample expresses a different functional form, which can then be represented as a feed-forward neural network with unknown parameters. More precisely, in the RUM framework presented in Section 2.1 there are three functions that we wish to approximate. The first one, $U(\cdot)$, can be straightforwardly replaced by a neural network. The two other functions, $\boldsymbol{\epsilon}(\cdot)$ and $\boldsymbol{\nu}(\cdot)$, are random and instead of approximating them directly, we propose to use a sample average approximation. More specifically, for some large K , we can informally write

$$\pi(\mathbf{x}, \mathbf{z}, A) \sim \frac{1}{K^2} \cdot \sum_{k_1=1}^K \sum_{k_2=1}^K \mathbf{1} \{U(\mathbf{x}, \boldsymbol{\epsilon}_{k_1}(\mathbf{x}), \mathbf{z}, \boldsymbol{\nu}_{k_2}(\mathbf{z})) > U(\mathbf{x}', \boldsymbol{\epsilon}_{k_1}(\mathbf{x}'), \mathbf{z}, \boldsymbol{\nu}_{k_2}(\mathbf{z})) \text{ , } \forall \mathbf{x}' \in A \setminus \mathbf{x}\} \text{ , } (1)$$

where, for each $k_1 \in [K]$, $\boldsymbol{\epsilon}_{k_1}(\cdot)$ denotes an independent sample of the random field $\boldsymbol{\epsilon}(\cdot)$. Analogously, for each $k_2 \in [K]$, $\boldsymbol{\nu}_{k_2}(\cdot)$ is an independent sample of the random field $\boldsymbol{\nu}(\cdot)$. Since $\boldsymbol{\epsilon}_{k_1}(\cdot)$ and $\boldsymbol{\nu}_{k_2}(\cdot)$ are now deterministic functions, we can approximate them using neural networks. In the remainder of this section, we formalize the class of choice models resulting from this combination of neural networks. We subsequently show in Section 3 that it approximates any RUM arbitrarily closely.

Feed-forward neural networks. We use feed-forward neural networks as building blocks to construct our model *architecture*, which refers to the combination of these neural networks. For our purposes, a feed-forward neural network is a function $N(\cdot) : \mathbb{R}^{d_{\text{input}}} \rightarrow \mathbb{R}^{d_{\text{output}}}$, where d_{input} is the size of the input and d_{output} the size of the output. For every scalar $M \geq 0$ and integers $\ell, w \geq 0$, let $\Theta_M^{\ell, w}$

be the class of feed-forward neural networks $N(\cdot) \in \Theta$ of depth ℓ and width w , whose weights have a 1-norm upper bounded by M at each node. We give a more formal account in Appendix A.1.

RUMnet architecture. Let $d = d_x + d_\epsilon + d_z + d_\nu$ be the dimension of the input vector to the utility function $U(\cdot)$ which governs the RUM framework. Additionally, let $K \geq 0$ be an integer that controls the number of samples we use to approximate the random fields. With this notation at hand, we introduce a RUMnet architecture, which is a family of neural networks, comprising of the following building blocks:

1. *Utility function:* There is a feed-forward neural network $N_U(\cdot) \in \Theta_M^{\ell,w}$ such that $N_U(\cdot)$ is a mapping from \mathbb{R}^d to \mathbb{R} that serves as an approximation of the function $U(\cdot)$.
2. *Unobserved product attributes:* For every $k_1 \in [K]$, there is a feed-forward neural network $N_{\epsilon_{k_1}}(\cdot) \in \Theta_M^{\ell,w}$ such that $N_{\epsilon_{k_1}}(\cdot)$ is a mapping from \mathbb{R}^{d_x} to \mathbb{R}^{d_ϵ} . Intuitively, each of these neural networks serves as an approximation to one sample of the random field $\epsilon(\cdot)$.
3. *Unobserved customer attributes:* For every $k_2 \in [K]$, there is a feed-forward neural network $N_{\nu_{k_2}}(\cdot) \in \Theta_M^{\ell,w}$ such that $N_{\nu_{k_2}}(\cdot)$ is a mapping from \mathbb{R}^{d_z} to \mathbb{R}^{d_ν} . Intuitively, each of these neural networks serves as an approximation to one sample of the random field $\nu(\cdot)$.

Consequently, we denote by $\mathcal{N}^d(K, \Theta_M^{\ell,w})$ the collection of all RUMnet architectures $(N_U(\cdot), \{N_{\epsilon_{k_1}}(\cdot)\}_{k_1=1}^K, \{N_{\nu_{k_2}}(\cdot)\}_{k_2=1}^K)$. The parameters of a given architecture are the number of samples of the SAA and the depth/width of each building block. The number of samples controls the latent (random) effects, whereas the size of each neural network determines the “degree of nonlinearity” expressed by the utility function.

RUMnet discrete choice model. We now specify the discrete choice model induced by any given RUMnet architecture $N = (N_U(\cdot), \{N_{\epsilon_{k_1}}(\cdot)\}_{k_1=1}^K, \{N_{\nu_{k_2}}(\cdot)\}_{k_2=1}^K) \in \mathcal{N}^d(K, \Theta_M^{\ell,w})$. For any choice event $(z, A) \in \mathcal{Z} \times 2^X$, we specify the probability $\pi_N^{\text{RUMnet}}(\mathbf{x}, z, A)$ that a customer with observable attributes z chooses $\mathbf{x} \in A$ as follows:

$$\pi_N^{\text{RUMnet}}(\mathbf{x}, z, A) = \frac{1}{K^2} \cdot \sum_{k_1=1}^K \sum_{k_2=1}^K \Pr_{\delta} \left[N_U \left(\mathbf{x}, N_{\epsilon_{k_1}}(\mathbf{x}), z, N_{\nu_{k_2}}(z) \right) + \delta_{\mathbf{x}} > N_U \left(\mathbf{x}', N_{\epsilon_{k_1}}(\mathbf{x}'), z, N_{\nu_{k_2}}(z) \right) + \delta_{\mathbf{x}'}, \forall \mathbf{x}' \in A \setminus \mathbf{x} \right],$$

where $\delta = \{\delta_{\mathbf{x}}\}_{\mathbf{x} \in A}$ is a sequence of independent real-valued random variables that follows the same distribution. Comparing the expression of $\pi_N^{\text{RUMnet}}(\cdot)$ with our sample average approximation (1), we have replaced the indicator with a probability distribution over δ . We will only require that this distribution has a strictly positive density on \mathbb{R} .² Nevertheless, in our implementation, we will

² As explained in Section 4.1, in the absence of the latter property, commonly used loss functions (e.g., log-likelihood) exhibit a gradient of zero with respect to the parameters of the neural network in a set of positive measure.

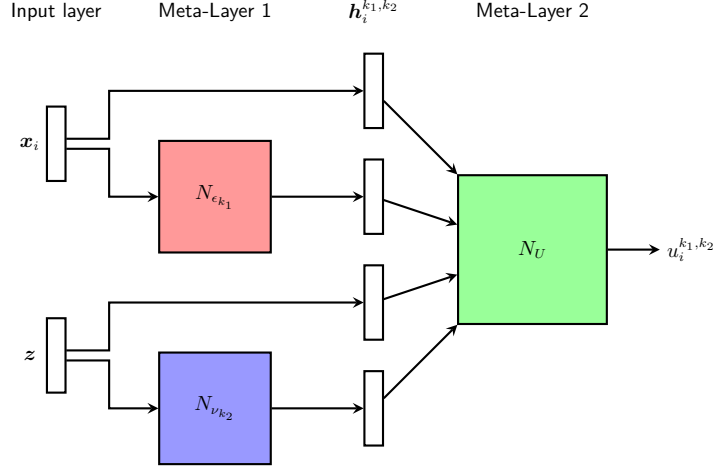


Figure 1 Illustration of the first two meta-layers. Note that we show the computation for one particular product attribute \mathbf{x}_i and sample (k_1, k_2) , but we apply the same transformation for each $\mathbf{x} \in A$ and $(k_1, k_2) \in K^2$.

assume that δ follows a standard Gumbel distribution, which amounts to replacing the “argmax” indicator with the “softmax” operation. This trick, often used in deep learning, allows us to estimate $\pi_N^{\text{RUMnet}}(\cdot)$ as a standard neural network, as we discuss next.

2.3. Interpretation as a neural network

For any given RUMnet architecture $N \in \mathcal{N}^d(K, \Theta_M^{\ell, w})$, we can interpret the computation of the probabilities $\{\pi_N^{\text{RUMnet}}(\mathbf{x}, \mathbf{z}, A)\}_{\mathbf{x} \in A}$ associated with a choice event (\mathbf{z}, A) as the output of a highly structured neural network. The input to this neural network consists of a vector formed by concatenating the observed product attributes $\mathbf{x}_1, \dots, \mathbf{x}_{|A|}$ together with the observed customer attributes \mathbf{z} . The computation graph comprises four “meta-layers”, which sequentially perform the following: (1) generating samples of unobserved attributes, (2) computing the alternative-specific utilities, (3) converting the utilities into probabilities, and (4) averaging. In Appendix A.2, we give a more precise mathematical description of these meta-layers. The design of the first two meta-layers carefully combines several feed-forward neural network building blocks, as illustrated in Figure 1. The third meta-layer simply consists of a softmax operator. The final meta-layer integrates the choice probabilities over all distinct samples of unobserved attributes. Figure 2 visualizes the overall architecture, while viewing the computation of $\pi_N^{\text{RUMnet}}(\cdot)$ as the output of a single neural network.

2.4. Connection with related models

Before we characterize the expressive power of RUMnets, we briefly demonstrate the ability of our model to capture various existing models as special cases. In its most basic form, the MNL model assumes that the utility for a product $\mathbf{x} \in \mathcal{X}$ is given by

$$U(\mathbf{x}) = \beta^T \mathbf{x} + \epsilon_{\mathbf{x}}, \quad (\text{MNL})$$

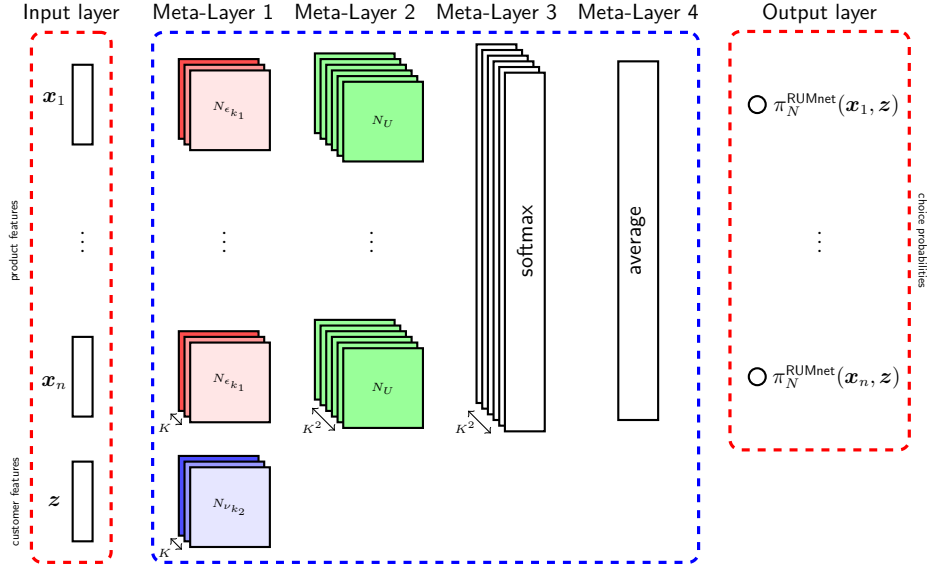


Figure 2 A RUMnet architecture $N = (N_U(\cdot), \{N_{\epsilon_{k_1}}(\cdot)\}_{k_1=1}^K, \{N_{\nu_{k_2}}(\cdot)\}_{k_2=1}^K)$.

where β is a vector of parameters and $\{\epsilon_x\}_{x \in A}$ is an i.i.d. sequence of standard Gumbel shocks. Note that under this linear specification of the utility, the MNL model cannot leverage the customer attributes z . To overcome this limitation, researchers often manually specify some non-linearity by introducing cross-terms in the utility function. A more recent approach to capture taste heterogeneity across individuals, proposed by Han et al. (2020), is to specify the utility as follows:

$$U(\mathbf{x}, \mathbf{z}) = \beta^T \mathbf{x} + N^{\text{TasteNet}}(\mathbf{z})^T \mathbf{x} + \epsilon_x, \quad (\text{TasteNet})$$

where $N^{\text{TasteNet}}(\cdot) : \mathbb{R}^{d_z} \rightarrow \mathbb{R}^{d_x}$ is a feed-forward neural network. Note that TasteNet can express non-linear transformations $N^{\text{TasteNet}}(\mathbf{z})$ of the customer attributes z . However, the additive term $N^{\text{TasteNet}}(\cdot)^T \mathbf{x}$ still assumes a very specific form for how the customer attributes interact with the product attributes. In fact, nothing prevents us from allowing the utility to be a general function of \mathbf{x} and \mathbf{z} , just as in the RUM framework. Perhaps the most natural approach is to take TasteNet a step further and define DeepMNL as a RUM where the utility is given by:

$$U(\mathbf{x}, \mathbf{z}) = N^{\text{DeepMNL}}(\mathbf{x}, \mathbf{z}) + \epsilon_x, \quad (\text{DeepMNL})$$

where $N^{\text{DeepMNL}}(\cdot) : \mathbb{R}^{d_x + d_z} \rightarrow \mathbb{R}$ is an arbitrary feed-forward neural network. Here, DeepMNL can be viewed as a special case of the RUMnet architecture in which there are no unobserved attributes ($K = 0$); several variants of DeepMNL have been proposed in the literature (Bentz and Merunka 2000, Sifringer et al. 2020, Wang et al. 2020). With respect to Figure 2, this approach consists in dropping the first meta-layer, and only keeping the second and third meta-layers. Since there is no latent heterogeneity, there is no need for the fourth (averaging) meta-layer either.

The above sequence of choice models illustrates a gradual increase of complexity and nonlinearity in the deterministic portion of the utility function, which can be conveniently expressed and estimated using neural networks. As highlighted by Train (2009), if the researcher could specify $N^{\text{DeepMNL}}(\mathbf{x}, \mathbf{z})$ “sufficiently that the remaining, unobserved portion of utility is essentially white noise”, then the DeepMNL approach would be ideal. However, regardless of how complex the deterministic portion of the utility is, DeepMNL and its variants are subject to the same restrictions as the MNL choice model. These approaches leave unexploited the latent heterogeneity that has received much of the attention in the literature on discrete choice modeling. Contrary to DeepMNL, our RUMnet architecture captures heterogeneity by incorporating unobserved product and customer attributes. The empirical (sample-based) distribution for these latent attributes endows RUMnets with a nearly universal expressive power, as established in the next section.

3. Expressive Power of RUMnets

In this section, we show that RUMnets tightly describe the class of all RUMs. In particular, we show that any RUM can be approximated arbitrarily closely by a RUMnet.

PROPOSITION 1. *For every RUM discrete choice model $\pi(\cdot)$ of dimension \mathbf{d} and for every $\eta > 0$, there exists a RUMnet architecture $N \in \mathcal{N}^{\mathbf{d}}(K, \Theta_M^{\ell, w})$ such that, for all choice events $(\mathbf{z}, A) \in \mathcal{Z} \times 2^{\mathcal{X}}$, $\max_{\mathbf{x} \in A} |\pi(\mathbf{x}, \mathbf{z}, A) - \pi_N^{\text{RUMnet}}(\mathbf{x}, \mathbf{z}, A)| \leq \eta$.*

To prove Proposition 1, we revisit the celebrated result of McFadden and Train (2000, Theorem 1) showing that *continuous mixtures* of MNL models uniformly approximate the class of RUMs. That said, Proposition 1 establishes a stronger property: the choice probabilities of RUMs are uniformly approximated by *finite mixtures* of MNLs on any choice event in the continuous domain. For this purpose, our proof extends the ideas in McFadden and Train (2000) by carefully combining a refined covering lemma with concentration bounds. At a high-level, the proof consists in showing that when we approximate the random utility function using feed-forward neural networks, the choice probabilities do not change much. Specifically, we analyze the likelihood of a “preference reversal” for every pair of alternatives (\mathbf{x}, \mathbf{z}) and $(\mathbf{x}', \mathbf{z})$ with $\mathbf{x} \neq \mathbf{x}'$ by controlling the variations of the utility function. Key to this analysis is the existence of a finite covering of $\mathcal{X}^2 \times \mathcal{Z}$ on which we can bound the errors incurred by our SAA approximation. The formal proof appears in Appendix B. Next, we establish that the reciprocal of Proposition 1 holds as well.

PROPOSITION 2. *For every RUMnet architecture $N \in \mathcal{N}^{\mathbf{d}}(K, \Theta_M^{\ell, w})$ and for every $\eta > 0$, there exists a RUM discrete choice model $\pi(\cdot)$ of dimension \mathbf{d} such that, for all choice events $(\mathbf{z}, A) \in \mathcal{Z} \times 2^{\mathcal{X}}$, $\max_{\mathbf{x} \in A} |\pi_N^{\text{RUMnet}}(\mathbf{x}, \mathbf{z}, A) - \pi(\mathbf{x}, \mathbf{z}, A)| \leq \eta$.*

The proof of Proposition 2 is straightforward: following the interpretation of our neural network architecture given in Section 2.4, RUMnet architectures directly represent the random choices of a utility-maximizing agent, while a small random perturbation of the RUMnet ensures that the regularity conditions of McFadden and Train (2000) are met.

4. Dealing with the Curse of Dimensionality

Given the expressive power of RUMnets demonstrated by Proposition 1, one important concern is the risk of overfitting, which could affect the model’s ability to generalise to new, previously unseen data. Hence, in this section, we provide theoretical guarantees on the out-of-sample error of the fitted RUMnets. More specifically, we provide an upper bound on the *generalization error*, which measures the degree of overfitting, i.e., it characterizes how the (out-of-sample) expected risk is related to the minimum (in-sample) empirical risk attained by our hypothesis class. We exploit this generalization error bound to establish a compact representation property, showing that any RUMnet architecture can be accurately represented using a relatively “small” number of samples.

4.1. Estimation framework

We formulate the estimation of the neural network of Section 2.3 in the standard Empirical Risk Minimization (ERM) framework; see Shalev-Shwartz and Ben-David (2014, Chap. 2) for further background. We assume that our data set is given by a sample of T i.i.d. observations $S = \{(\mathbf{y}_1, \mathbf{z}_1, A_1), \dots, (\mathbf{y}_T, \mathbf{z}_T, A_T)\}$, where (\mathbf{z}_t, A_t) is the t -th choice event and $\mathbf{y}_t \in A_t$ is the product picked by the corresponding customer. To ease the exposition, we further assume that the assortments have a uniform cardinality $|A_t| = \kappa$ for all $t \in [T]$. Notation-wise, \mathcal{D} stands for the marginal distribution of each observation in the sample, i.e., $S \sim \mathcal{D}^T$. By a slight abuse of notation, we sometimes use $(\mathbf{z}_t, A_t) \sim \mathcal{D}$ (instead of $(\mathbf{y}_t, \mathbf{z}_t, A_t) \sim \mathcal{D}$) to indicate that the choice event is generated according to \mathcal{D} . We do not impose the so-known *realizability assumption*, meaning that our modeling approach can be misspecified, i.e., we do not assume that \mathcal{D} is attained by some RUM.

We proceed by formulating our estimation criterion. As an input to our estimation procedure, we specify the parameters $\mathbf{d}, K, w, \ell, M \geq 0$ so that we restrict our estimation procedure to the hypothesis class $\mathcal{N}^{\mathbf{d}}(K, \Theta_M^{\ell, w})$ of RUMnet architectures. Our estimator is based on the ERM principle with respect to the negative log-likelihood loss function. Specifically, given a sample S and a discrete choice model $\pi(\cdot)$, we let $L_S(\pi)$ be the empirical negative log-likelihood, namely

$$L_S(\pi) = -\frac{1}{T} \cdot \sum_{t=1}^T \log(\pi(\mathbf{y}_t, \mathbf{z}_t, A_t)) . \quad (2)$$

With this definition, our approach is to choose the RUMnet architecture that minimizes the above empirical loss over all RUMnet architectures. Formally, $N_S^{\text{ERM}} = \arg \min_{N \in \mathcal{N}(\mathbf{d}, K, \Theta_{v, M})} L_S(\pi_N)$. Note

that the fitted RUMnet architecture N_S^{ERM} is a function of the observed (random) sample S . Additionally, let $\pi_S^{\text{ERM}}(\cdot)$ be the associated discrete choice model, i.e., $\pi_S^{\text{ERM}}(\cdot) = \pi_{N_S^{\text{ERM}}}^{\text{RUMnet}}(\cdot)$. It is worth highlighting that the ERM principle is equally applicable to other loss functions such as mean-squared error or accuracy. Nonetheless, our analysis will focus on log-likelihood-based estimation, in accordance with the fitting procedure used for other classes of choice models. From a practical perspective, estimating a RUMnet discrete choice model using the ERM principle reduces to training a neural network for multi-label classification. The log-likelihood loss function is often referred to as the cross-entropy loss in the ML practice. Thus, the ERM rule can be implemented using graph optimization and automatic differentiation tools such as Tensorflow, PyTorch, Keras, etc.

4.2. Learning error guarantees and compact representation

We define the true error as the expected out-of-sample loss where the expectation is taken over the unknown distribution \mathcal{D} . Specifically, for any discrete choice model $\pi(\cdot)$ let $L_{\mathcal{D}}^{\text{true}}(\pi) = \mathbb{E}_{S' \sim \mathcal{D}^T}[L_{S'}(\pi)]$. Note that this is ideally what we want to minimize. However, since we cannot directly measure out-of-sample performance, as the distribution is unknown, we minimize the empirical error defined in Equation (2). The next claim quantifies the gap between these errors.

PROPOSITION 3. *With probability at least $(1 - \delta)$, the sampled training set S satisfies*

$$L_{\mathcal{D}}^{\text{true}}(\pi_S^{\text{ERM}}) \leq L_S(\pi_S^{\text{ERM}}) + c_1 \cdot \frac{\kappa \cdot \sqrt{\kappa}}{\sqrt{T}} \cdot e^{2M} M^\ell + 4 \cdot c_2 \cdot \sqrt{\frac{2 \cdot \ln(4/\delta)}{T}}.$$

The proof, presented in Appendix C.1, is based on notions of Rademacher calculus applied to the RUMnet architecture. As common for neural networks, the error bound of Proposition 3 indicates an exponential dependence on depth ℓ of the neural network, as well as the bound M on the ℓ_1 -norm of its weight parameters. Yet, this bound on the generalization error reveals two noteworthy properties. First, our bound does not depend on the number of samples K . One potential interpretation is that the complexity added to the hypothesis class by increasing the sample size K might not generate as much over-fitting as other dimensions of the RUMnet architecture (in a worst-case asymptotic sense). Second, it is worth noticing a subquadratic dependence $O(\kappa^{\frac{3}{2}} T^{-\frac{1}{2}})$ on the number of choice alternatives κ , which is significant better than the existing bound of $\Omega(\kappa^{\ell/2} T^{-\frac{1}{2}})$ by Wang et al. (2021). For another comparison point, choice modeling can be viewed as a structured form of classification problem. In this context, classical Rademacher complexity bounds on margin-based learning for multi-label classification have a quadratic scaling $O(\kappa^2 T^{-\frac{1}{2}})$ (Koltchinskii and Panchenko 2000, Cortes et al. 2013, Mohri et al. 2018), unless further restrictions are imposed on the hypothesis class or more sophisticated analytical methods are used.

Building on Proposition 3, we next explore the number of samples K required in the RUMnet architecture to accurately describe any RUMnet choice model for a fixed data distribution. Our next claim shows that, with a small $O(\epsilon)$ loss in accuracy in terms of expected KL-divergence, the number of samples K can be chosen in the order of $O(\frac{1}{\epsilon^2} \text{poly}(\log \frac{1}{\epsilon}, \ell, \kappa, e^M))$. This finding suggests that the latent heterogeneity of the model should be commensurate to the complexity of the feed-forward neural network building blocks of our architecture.

PROPOSITION 4. *For every neural network architecture $N \in \mathcal{N}^d(K, \Theta_M^{\ell, w})$, let $N' \in \mathcal{N}^d(K', \Theta_M^{\ell, w})$ be the (random) neural network architecture obtained from N by taking $K' = \lceil \frac{1}{2\epsilon^2} \cdot \log \delta \cdot (\kappa e^{2M})^2 \log(\lceil \frac{16}{\max\{c_1^2, c_2^2\} \cdot \epsilon^2} \kappa^3 e^{4M} M^{2\ell} \rceil) \rceil$ samples of the unobserved attributes $\{N_{\epsilon_{k_1}}(\cdot)\}_{k_1=1}^K$ and $\{N_{\nu_{k_2}}(\cdot)\}_{k_2=1}^K$ uniformly at random with replacement. Then, with probability at least $1 - \delta$,*

$$\mathbb{E}_{(\mathbf{z}, A) \sim \mathcal{D}} [\text{KL}(\pi_{N'}^{\text{RUMnet}}(\cdot, \mathbf{z}, A) \mid \pi_N^{\text{RUMnet}}(\cdot, \mathbf{z}, A))] \leq 3\epsilon.$$

This claim can be viewed as the counterpart of Theorem 4 in the paper by Chierichetti et al. (2018) for feature-dependent choice models in the continuous domain, rather than the discrete domain. The proof appears in Appendix C.2 and combines Proposition 3 with concentration bounds.

5. Numerical Experiments

We test the predictive accuracy of RUMnets against a comprehensive set of benchmarks on two real-world datasets, which reflect complementary choice prediction settings.

5.1. Benchmarks and implementation specifications

We implement various choice models and classification algorithms proposed in previous literature. The first set of benchmarks comprises the MNL model and the two neural network-based extensions, TasteNet and DeepMNL, which we presented in Section 2.4. While the MNL model specifies a linear utility function, the subsequent benchmarks capture nonlinear effects of increasing complexity. From an implementation perspective, we formulate each of these models as a neural network with a softmax prediction layer. In addition, we test two model-free benchmarks that treat the choice prediction task as a multi-label classification problem and forego any additional structure on the probabilistic choices: (1) *Random Forest (RF)*: We train a variant of the random forests for choice prediction recently proposed by Chen et al. (2019) and Chen and Mišić (2020). Importantly, these papers focus on a different observational setting, where the assortment composition varies but each product’s attributes are essentially fixed. Due to contextual variations in product and customer attributes, we implement a featurized version of this methodology, which was suggested by Chen et al. (2019). We note that the optimization-based estimation methods developed by Chen and Mišić (2020) are not easily applicable in this setting. (2) *Vanilla Neural Network (VNN)*: We train a naive

feed-neural neural network. The input is the concatenation of all product and customer attributes. The output is a vector of length $|A|$ that represents the utility of each choice alternative. This output is then passed through a softmax layer to compute the corresponding choice probabilities.

Except for the random forest model, we implement all other benchmarks using Keras. Appendix D.1 details our approach for estimating the neural networks-based models. A code snippet is provided to illustrate the ease of implementation using Keras. We test different complexities for the building-block neural networks. In particular, for each method, we experiment with $(\ell, w) \in \{(3, 10), (5, 20), (10, 30)\}$, where recall that ℓ denotes the depth of the network and w its width.³ For our RUMnet architecture, we also test out different number of samples $K \in \{5, 10\}$ controlling for the latent heterogeneity of customers and products. We also test the DeepMNL model of Section 2.4, which is similar in spirit to a RUMnet model that does not capture any latent heterogeneity, i.e., $K = 1$. Note that when, in addition, $(\ell, w) = (0, 0)$, the DeepMNL coincides with the MNL model. For RFs, we vary the number of trees in the forest in $\{50, 100, 200, 400\}$ and the maximum tree depth in $\{5, 10, 20\}$; we then pick the forest with the best loss on the validation set.

We use 10-fold cross-validation and report the averaged log-likelihood loss and classification over the ten splits. We use a 70/15/15 split for the train/validation/test sets respectively. Recall that the log-likelihood loss was defined in Equation (2). Moreover, we define the *accuracy* as the percentage of correct predictions for the chosen alternative.

5.2. Case studies

The first dataset (Swissmetro data) consists of responses to a survey in Switzerland to assess the potential demand for a new mode of public transportation, called Swissmetro. The alternatives include Swissmetro, Train or Car ($\kappa = 3$), and the number of observations in the data is in the order of 10K. The second one (Expedia data) is a larger dataset. This dataset counts around 275K distinct search queries, 35 hotel features, and 56 customer and search features. This setting mirrors large-scale transaction data with assortments formed by many distinct alternatives ($\kappa = 38$). More details on each dataset are presented in Appendices D.3 and D.4.

The predictive performance of the models is reported in Table 1. RUMnet emerges as the most predictive method out of all benchmarks. All models significantly outperform the MNL benchmark in terms of log-likelihood loss and prediction accuracy. The gaps of log-likelihoods exceed 20% in the Swissmetro dataset and is in the order of 16% for the Expedia dataset, thereby indicating that a linear utility-based model is too restrictive to accurately predict choices in this setting. Turning our

³ We omit certain instantiations of (ℓ, w) if the corresponding running times are prohibitive, or if the number of parameters becomes excessive.

Table 1 Predictive performance of different models

Model				Swissmetro						Expedia					
				Log-likelihood loss			Accuracy			Log-likelihood loss			Accuracy		
Type	(ℓ, w)	K	Train	Val	Test	Train	Val	Test	Train	Val	Test	Train	Val	Test	
MNL	-	-	0.828	0.824	0.825	0.624	0.625	0.625	2.692	2.691	2.692	0.208	0.207	0.208	
TasteNet	(3,10)	-	0.506	0.612	0.616	0.784	0.746	0.746	2.608	2.610	2.611	0.230	0.230	0.229	
	(5,20)	-	0.428	0.589	0.602	0.819	0.762	0.755	2.602	2.609	2.610	0.232	0.230	0.230	
	(10,30)	-	0.409	0.588	0.582	0.821	0.766	0.766	2.605	2.611	2.613	0.231	0.230	0.229	
DeepMNL	(3,10)	-	0.500	0.612	0.629	0.787	0.745	0.734	2.559	2.562	2.564	0.238	0.237	0.237	
	(5,20)	-	0.390	0.575	0.592	0.837	0.771	0.764	2.541	2.550	2.551	0.242	0.239	0.239	
	(10,30)	-	0.375	0.562	0.575	0.842	0.774	0.771	2.537	2.549	2.551	0.242	0.239	0.239	
RUMnet	(3,10)	5	0.341	0.563	0.574	0.857	0.771	0.772	2.523	2.536	2.539	0.245	0.242	0.242	
	(3,10)	10	0.316	0.543	0.548	0.867	0.781	0.777	2.507	2.532	2.535	0.248	0.244	0.242	
	(5,20)	5	0.327	0.521	0.543	0.864	0.790	0.783	2.512	2.530	2.533	0.248	0.243	0.243	
	(5,20)	10	0.288	0.512	0.523	0.882	0.796	0.791	2.510	2.530	2.532	0.248	0.244	0.244	
VNN	(3,10)	-	0.451	0.588	0.588	0.810	0.758	0.756	3.328	3.349	3.348	0.248	0.244	0.244	
	(5,20)	-	0.424	0.570	0.580	0.824	0.765	0.758	3.233	3.275	3.275	0.093	0.086	0.086	
	(10,30)	-	0.425	0.593	0.586	0.817	0.750	0.749	3.306	3.337	3.336	0.081	0.077	0.077	
RF	-	-	0.186	0.536	0.537	1.000	0.774	0.774	1.894	3.203	3.203	1.000	0.175	0.176	

attention to RUMnets, we see that increasing the complexity of the networks improves the performance of RUMnets. For instance, for the Swissmetro dataset, fixing $K = 5$, the log-likelihood loss decreases by about 4% when going from $(\ell, w) = (3, 10)$ to $(\ell, w) = (5, 20)$. This improvement shows the gain in prediction accuracy that can be imputed to a complex nonlinear utility function. Interestingly, we observe comparable gains when increasing the number of samples K , which indicate the value-added of latent heterogeneity. For instance, comparing DeepMNLs with RUMnets on the Expedia dataset, we see that the incorporation of latent heterogeneity (i.e., $K \in \{5, 10\}$) benefits the out-of-sample log-likelihood by nearly 2%. This difference is significant, albeit more marginal than that on the Swissmetro dataset. Interestingly, we note that augmenting the complexity (ℓ, w) of DeepMNLs from $(5, 20)$ to $(10, 30)$ does not yield any marginal improvement. Hence, it is not possible to “make up” for the lack of latent heterogeneity using a more complex utility function. These observations are validated by our controlled synthetic experiments in Appendix D.2, where we test out different specifications of the utility function as the ground truth.

Comparing the neural network-based methods, we observe that, at equal feed-forward neural network complexity (ℓ, w) , TasteNet and VNN obtain relatively similar performances to DeepMNLs on the Swissmetro dataset; VNN has a small edge on the other two approaches. This is surprising as the VNN method ignores the structure of the choice prediction problem. That said, none of these models capture any latent heterogeneity, which might explain the superior performance of RUMnets. Despite being on par with RUMnets on the Swissmetro dataset, the model-free methods – RFs and VNNs – have a poor performance on the Expedia dataset. We note that RFs suffer

from a high level of overfitting, as indicated by the gap of performance on our training and test data.⁴ This striking phenomenon might be related to the large number of distinct alternatives and product attributes of Expedia data. Indeed, for such model-free approaches, an explosion of the number of parameters seems unavoidable as the input dimension increases (see Table EC.2). We back this explanation by conducting controlled synthetic experiments in Appendix D.6.

5.3. Visualization

Neural networks are often viewed as “black-box” tools that are hard to interpret. Hence, it is important to explore what type of substitution patterns are captured by the fitted RUMnets and contrast them with other methods. As a first step, we visualize how the RUMnet predictions vary as a function of the price, which is arguably one of the most important operational dimension, using the Swissmetro dataset. In order to visualize how RUMnets predict the customers’ substitution patterns, we use the K -means method to determine a balanced partition of the customer features and subsequently define the centroid of each cluster as a distinct customer type. Figure 3 plots the predicted choice probabilities of each customer types as a function of the Swissmetro cost. Our clustering reveals three distinct choice behaviors: Customer 1 is mostly price insensitive and chooses the Swissmetro with high probability even when increasing its cost. Both Customers 2 and 3 are price sensitive and choose the Swissmetro option when its cost is low enough. Interestingly, they differ in what they substitute to when the cost of the Swissmetro is too high: Customer 2 chooses the Train option whereas Customer 3 chooses the Car option.

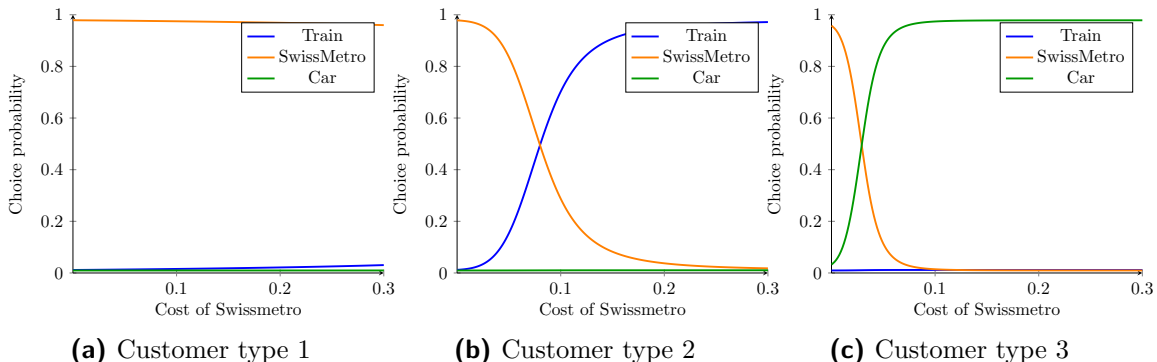


Figure 3 Different substitution patterns predicted by DeepMNL with parameters $(\ell, w) = (2, 5)$.

For all customer types, the choice probability of the Swissmetro decreases with its cost. This shows that RUMnets capture realistic substitution patterns with respect to price. Note that in practice, these relationships may or may not be observed due to a variety of issues, including

⁴Since the hyper-parameters of RFs are tuned using the validation set, our estimation method enables selecting smaller tree depths or fewer trees in the forest. Yet, these choices do not result in better out-of-sample performance.

the presence of endogeneity and overfitting. In fact, in the case of random forests, the predicted choice probability for Swissmetro does not always decrease as its price increases. Figure EC.4 in Appendix D.5 illustrates this phenomenon. This finding shows that model-free methods may capture unrealistic dependencies on product attributes, in spite of their strong predictive accuracy.

6. Conclusion

In this paper, we introduce a new class of neural network-based choice models. Our neural network architecture, RUMnet, provides an efficient approximation of RUM discrete choice models. Unlike traditional RUMs, which rely on specific structural and distributional assumptions, RUMnets leverage the universality of feed-forward neural networks to learn the structure of the random utility function from data. Moreover, our method is practical as RUMnets can be trained using existing open-source libraries. By satisfying the RUM principle, we believe that our structured machine learning approach yields better generalization to high-dimensional inputs than other model-free methods, as illustrated by our numerical findings. This work opens several intriguing research directions. For instance, it might be possible to exploit the flexibility of the RUMnet architecture for more complicated choice estimation problems such as multi-item and dynamic discrete choice. Another important research avenue is to develop practical algorithms for decision problems such as assortment optimization or pricing under this choice model.

References

- Bartlett, Peter L, Shahar Mendelson. 2002. Rademacher and gaussian complexities: Risk bounds and structural results. *Journal of Machine Learning Research* **3**(Nov) 463–482.
- Bentz, Yves, Dwight Merunka. 2000. Neural networks and the multinomial logit for brand choice modelling: a hybrid approach. *Journal of Forecasting* **19**(3) 177–200.
- Berbeglia, Gerardo. 2018. The generalized stochastic preference choice model. *arXiv preprint arXiv:1803.04244* .
- Bierlaire, M. 2018. Swissmetro. URL: https://transpor.epfl.ch/documents/technicalReports/CS_SwissmetroDescription.pdf .
- Chen, Ningyuan, Guillermo Gallego, Zhuodong Tang. 2019. The use of binary choice forests to model and estimate discrete choices. Available at SSRN 3430886 .
- Chen, Yi-Chun, Velibor Mišić. 2020. Decision forest: A nonparametric approach to modeling irrational choice. Available at SSRN 3376273 .
- Chierichetti, Flavio, Ravi Kumar, Andrew Tomkins. 2018. Discrete choice, permutations, and reconstruction. *Proceedings of the Twenty-Ninth Annual ACM-SIAM Symposium on Discrete Algorithms*. SIAM, 576–586.

-
- Cortes, Corinna, Mehryar Mohri, Afshin Rostamizadeh. 2013. Multi-class classification with maximum margin multiple kernel. *International Conference on Machine Learning*. PMLR, 46–54.
- Farias, Vivek F, Srikanth Jagabathula, Devavrat Shah. 2013. A nonparametric approach to modeling choice with limited data. *Management science* **59**(2) 305–322.
- Feldman, Jacob, Dennis Zhang, Xiaofei Liu, Nannan Zhang. 2018. Customer choice models versus machine learning: Finding optimal product displays on alibaba. *Available at SSRN 3232059* .
- Gabel, Sebastian, Artem Timoshenko. 2021. Product choice with large assortments: A scalable deep-learning model. *Management Science* .
- Han, Yafei, Christopher Zegras, Francisco Camara Pereira, Moshe Ben-Akiva. 2020. A neural-embedded choice model: TasteNet-MNL modeling taste heterogeneity with flexibility and interpretability. *arXiv:2002.00922* .
- Hornik, Kurt. 1991. Approximation capabilities of multilayer feedforward networks. *Neural networks* **4**(2) 251–257.
- Hornik, Kurt, Maxwell Stinchcombe, Halbert White. 1989. Multilayer feedforward networks are universal approximators. *Neural networks* **2**(5) 359–366.
- Jiang, Zhaohui Zoey, Jun Li, Dennis Zhang. 2020. A high-dimensional choice model for online retailing. *Available at SSRN 3687727* .
- Koltchinskii, Vladimir, Dmitriy Panchenko. 2000. Rademacher processes and bounding the risk of function learning. *High dimensional probability II*. Springer, 443–457.
- Luce, R.D. 1959. *Individual choice behavior: A theoretical analysis*. Wiley.
- Maurer, Andreas. 2016. A vector-contraction inequality for rademacher complexities. *International Conference on Algorithmic Learning Theory*. Springer, 3–17.
- McFadden, Daniel. 1974. Conditional logit analysis of qualitative choice behavior. *Frontiers in Econometrics* **2** 105–142.
- McFadden, Daniel, Kenneth Train. 2000. Mixed mnl models for discrete response. *Journal of applied Econometrics* **15**(5) 447–470.
- Mohri, Mehryar, Afshin Rostamizadeh, Ameet Talwalkar. 2018. *Foundations of machine learning*. MIT press.
- Rosenfeld, Nir, Kojin Oshiba, Yaron Singer. 2020. Predicting choice with set-dependent aggregation. *International Conference on Machine Learning*. PMLR, 8220–8229.

- Rusmevichientong, Paat, Benjamin Van Roy, Peter W Glynn. 2006. A nonparametric approach to multiproduct pricing. *Operations Research* **54**(1) 82–98.
- Shalev-Shwartz, Shai, Shai Ben-David. 2014. *Understanding machine learning: From theory to algorithms*. Cambridge university press.
- Sifringer, Brian, Virginie Lurkin, Alexandre Alahi. 2020. Enhancing discrete choice models with representation learning. *Transportation Research Part B: Methodological* **140** 236–261.
- Train, Kenneth E. 2009. *Discrete Choice Methods with Simulation*. Cambridge University Press, Cambridge, United Kingdom.
- Wang, Shenhao, Baichuan Mo, Jinhua Zhao. 2020. Deep neural networks for choice analysis: Architecture design with alternative-specific utility functions. *Transportation Research Part C: Emerging Technologies* **112** 234–251.
- Wang, Shenhao, Qingyi Wang, Nate Bailey, Jinhua Zhao. 2021. Deep neural networks for choice analysis: A statistical learning theory perspective. *Transportation Research Part B: Methodological* **148** 60–81.
- Williams, H.C.W.L. 1977. On the formation of travel demand models and economic evaluation measures of user benefit. *Environment and Planning A* **3**(9) 285–344.
- Wolf, Michael M. 2018. *Mathematical foundations of supervised learning*.
- Wong, Melvin, Bilal Farooq. 2019. Reslogit: A residual neural network logit model. *arXiv:1912.10058* .

This page is intentionally blank. Proper e-companion title page, with INFORMS branding and exact metadata of the main paper, will be produced by the INFORMS office when the issue is being assembled.

Online Appendix

Representing Random Utility Choice Models with Neural Networks

Appendix A: Additional material for Section 2

A.1. Feed-forward neural networks

A feed-forward neural network is specified by a directed acyclic graph, $G = (V, E)$. Each edge $e \in E$ is associated with a weight $w_e \in \mathbb{R}$. Each node of the graph, called a neuron, is associated with an activation function $\sigma : \mathbb{R} \rightarrow \mathbb{R}$. Each edge in the graph links the output of some neuron to the input of another neuron. The input of a neuron is obtained by taking a weighted sum of the outputs of all neuron connected to it. We assume that the nodes are organized in layers, i.e. the set of nodes is partitioned in disjoint subsets $V = \cup_{t=0}^T V_t$, such that every edge in E connects some node in V_{t-1} to some node in V_t , for some $t \in [T]$. We denote by $v_{i,t} \in V_t$ the i^{th} neuron of the t^{th} layer. Moreover, for any input \mathbf{x} to the network and $v_{i,t} \in V_t$, we let $o_{i,t}(\mathbf{x})$ (resp. $a_{i,t}(\mathbf{x})$) denotes the output (resp. input) of $v_{i,t}$. Then,

$$a_{i,t+1} = \sum_{j:e=(v_{j,t},v_{i,t+1}) \in E} w_e \cdot o_{j,t}(\mathbf{x}),$$

and

$$o_{i,t+1}(\mathbf{x}) = \sigma(a_{i,t+1}(\mathbf{x})).$$

The first layer V_0 is called the input layer and the last layer V_T is the output layer which often contains a single neuron. The layers V_1, \dots, V_{T-1} are called the hidden layers. We refer to T as the depth of the network. The width of the network is $\max_{t=1, \dots, T-1} |V_t|$ and its size is $|V|$. Figure EC.1 illustrates a feed-forward network of depth 2. Feed-forward neural networks are able to capture complex non-linear patterns and have been shown to be a class of universal approximators. That is, under mild conditions, the class of neural networks $\bigcup_{k \geq 1} \Theta_k^{1,k}$ with only one hidden layer and one output unit is dense in the space of continuous functions over a compact domain X , e.g., this result holds for any continuous, bounded and non-constant activation function (Hornik et al. 1989, Hornik 1991).

A.2. Interpretation of RUMnet as a single neural network

Recall that we can write $N = (N_U(\cdot), \{N_{\epsilon_{k_1}}(\cdot)\}_{k_1=1}^K, \{N_{\nu_{k_2}}(\cdot)\}_{k_2=1}^K)$. The distribution $\{\pi_N^{\text{RUMnet}}(\mathbf{x}, \mathbf{z}, A)\}_{\mathbf{x} \in A}$ is the output of a computation graph comprising four “meta-layers”, which are detailed below:

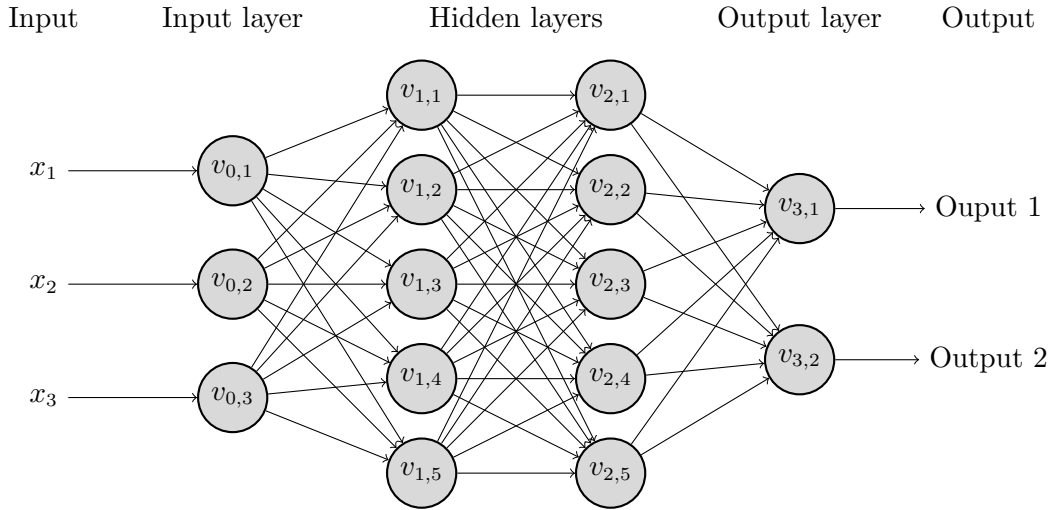


Figure EC.1 An example of feed-forward neural network.

- *Input vector.* Let $\mathbf{x}_1, \dots, \mathbf{x}_{|A|}$ be an arbitrary numbering of the alternatives in the assortment A . The input to our neural network is the vector $(\bigoplus_{i=1}^{|A|} \mathbf{x}_i) \oplus \mathbf{z}$ formed by concatenating the observed product attributes $\mathbf{x}_1, \dots, \mathbf{x}_{|A|}$ together with the observed customer attributes \mathbf{z} .

- *Meta-layer 1: Computing the unobserved attributes.* In the first layer, for each $i \in \{1, \dots, |A|\}$ and $k_1 \in [K]$, \mathbf{x}_i is passed through $N_{\epsilon_{k_1}}(\cdot)$ and, for each $k_2 \in [K]$, \mathbf{z} is passed through $N_{\nu_{k_2}}(\cdot)$. Here, $N_{\epsilon_{k_1}}(\mathbf{x}_i)$ can be thought of as the k_1 -th sample of unobserved product attributes for the alternative \mathbf{x}_i , while $N_{\nu_{k_2}}(\mathbf{z})$ is the k_2 -th sample of unobserved attributes for customer \mathbf{z} . In what follows, we write $\mathbf{h}_i^{k_1, k_2} = \mathbf{x}_i \oplus N_{\epsilon_{k_1}}(\mathbf{x}_i) \oplus \mathbf{z} \oplus N_{\nu_{k_2}}(\mathbf{z}) \in \mathbb{R}^d$ for the intermediate variables, i.e., the output of the first meta-layer and input to the second layer.

- *Meta-layer 2: Computing the utilities.* For each $i \in \{1, \dots, |A|\}$ and $(k_1, k_2) \in [K^2]$, $\mathbf{h}_i^{k_1, k_2}$ is passed through $N_U(\cdot)$. The resulting quantity $u_i^{k_1, k_2} = N_U(\mathbf{h}_i^{k_1, k_2})$ stands for the utility of the choice alternative \mathbf{x}_i for the sample (k_1, k_2) . The output of this second meta-layer is $\{\bigoplus_{i=1}^{|A|} u_i^{k_1, k_2}\}_{(k_1, k_2) \in [K^2]}$.

- *Meta-layer 3: Computing the induced probabilities.* Next, the utilities are converted into probabilities using a softmax layer. More precisely, for each $i \in \{1, \dots, |A|\}$ and $(k_1, k_2) \in [K^2]$, we let $\pi_i^{k_1, k_2} = e^{u_i^{k_1, k_2}} / (\sum_{j=1}^{|A|} e^{u_j^{k_1, k_2}})$.

- *Meta-layer 4: Averaging.* For each $i \in \{1, \dots, |A|\}$, the final output of the neural network is simply an average over all samples, yielding the choice probabilities $\pi_N^{\text{RUMnet}}(\mathbf{x}_i, \mathbf{z}, A) = \frac{1}{K^2} \cdot \sum_{k_1, k_2} \pi_i^{k_1, k_2}$.

Appendix B: Proofs of Section 3

B.1. A preliminary result

From the RUM framework, recall that we are interested in the ordering of the utilities for different alternatives. Indeed, for $\mathbf{x} \neq \mathbf{x}'$, $U(\mathbf{x}, \epsilon(\mathbf{x}), \mathbf{z}, \nu(\mathbf{z})) \geq U(\mathbf{x}', \epsilon(\mathbf{x}'), \mathbf{z}, \nu(\mathbf{z}))$ implies that \mathbf{x} is preferred

to \mathbf{x}' . The following lemma shows that it is sufficient to approximate $U(\cdot)$ on the finite covering C in order to capture the desired ordering relations of all possible pairs $(\mathbf{x}, \mathbf{x}') \in \mathcal{X}^2$ and customer attribute \mathbf{z} with high probability. Throughout our analysis, the space of product and customer attributes is endowed with the ℓ_∞ -norm unless stated otherwise.

LEMMA EC.1 (Part of Theorem 1 in McFadden and Train 2000). *For every $\eta > 0$, there exists a finite covering $(B(c, \delta(c)))_{c \in C}$ with centers $C \subset \mathcal{X}^2 \times \mathcal{Z}$, radii $(\delta(c))_{c \in C} > 0$, and integers $(n(c))_{c \in C}$ such that, given a fixed $c = (\hat{\mathbf{x}}, \hat{\mathbf{x}}', \hat{\mathbf{z}}) \in C$, with probability at least $1 - 3\eta/4\kappa$, we have for all $(\mathbf{x}, \mathbf{x}', \mathbf{z}) \in \mathcal{X}^2 \times \mathcal{Z}$ in the neighborhood of $(\hat{\mathbf{x}}, \hat{\mathbf{x}}', \hat{\mathbf{z}})$ that:*

1. $|U(\mathbf{x}, \boldsymbol{\epsilon}(\mathbf{x}), \mathbf{z}, \boldsymbol{\nu}(\mathbf{z})) - U(\hat{\mathbf{x}}, \boldsymbol{\epsilon}(\hat{\mathbf{x}}), \hat{\mathbf{z}}, \boldsymbol{\nu}(\hat{\mathbf{z}}))| \leq 1/n(c)$,
2. $|U(\mathbf{x}', \boldsymbol{\epsilon}(\mathbf{x}'), \mathbf{z}, \boldsymbol{\nu}(\mathbf{z})) - U(\hat{\mathbf{x}}', \boldsymbol{\epsilon}(\hat{\mathbf{x}}'), \hat{\mathbf{z}}, \boldsymbol{\nu}(\hat{\mathbf{z}}))| \leq 1/n(c)$.
3. $|U(\mathbf{x}, \boldsymbol{\epsilon}(\mathbf{x}), \mathbf{z}, \boldsymbol{\nu}(\mathbf{z})) - U(\mathbf{x}', \boldsymbol{\epsilon}(\mathbf{x}'), \mathbf{z}, \boldsymbol{\nu}(\mathbf{z}))| \geq 5/n(c)$

The above result, which we formalized, is the main step in the proof of the celebrated result of [McFadden and Train \(2000\)](#) showing that continuous mixtures of MNL models uniformly approximate the class of RUMS. The proof of this result exploits the uniform continuity of $U(\cdot)$, $\boldsymbol{\epsilon}(\mathbf{x})$ and $\boldsymbol{\nu}(\mathbf{z})$ for all $(\mathbf{x}, \mathbf{z}) \in \mathcal{X} \times \mathcal{Z}$. For completeness, the proof of Lemma EC.1 is given below; note that the statement of this result is implicit in [McFadden and Train \(2000\)](#), who base their analysis on slightly weaker properties of the covering.

Proof. Recall that $\boldsymbol{\epsilon}(\cdot)$ and $\boldsymbol{\nu}(\cdot)$ are random fields over \mathcal{X} and \mathcal{Z} respectively. For analysis purposes, we explicit this randomness. In particular, we introduce a fundamental probability space $(\Omega, \mathcal{W}, \Pr_\omega)$ and denote by $\boldsymbol{\epsilon}(w, \mathbf{x})$ (resp. $\boldsymbol{\nu}(w, \mathbf{z})$) a particular realization of $\boldsymbol{\epsilon}(\mathbf{x})$ (resp. $\boldsymbol{\nu}(\mathbf{z})$). For ease of notation, we let for $(w, \mathbf{x}, \mathbf{z}) \in \Omega \times \mathcal{X} \times \mathcal{Z}$,

$$F(w, \mathbf{x}, \mathbf{z}) = U(\mathbf{x}, \boldsymbol{\epsilon}(w, \mathbf{x}), \mathbf{z}, \boldsymbol{\nu}(w, \mathbf{z})).$$

Recall that for all choice event (\mathbf{z}, A) and $\mathbf{x} \in A$, we have

$$\pi(\mathbf{x}, \mathbf{z}, A) = \Pr_\omega[F(w, \mathbf{x}, \mathbf{z}) > F(w, \mathbf{x}', \mathbf{z}), \forall \mathbf{x}' \in A \setminus \mathbf{x}].$$

1. *Utility is sufficiently different for different alternatives.* For every $(\mathbf{x}, \mathbf{x}', \mathbf{z}) \in \mathcal{X}^2 \times \mathcal{Z}$ and $n \in \mathbb{N}_+$, let

$$\Omega_n(\mathbf{x}, \mathbf{x}', \mathbf{z}) = \{\omega \in \Omega : |F(\omega, \mathbf{x}, \mathbf{z}) - F(\omega, \mathbf{x}', \mathbf{z})| \geq 7/n\}.$$

The continuity of $U(\cdot)$ and the measurability of the random fields $\boldsymbol{\epsilon}(\cdot)$ and $\boldsymbol{\nu}(\cdot)$ implies that $\Omega_n(\mathbf{x}, \mathbf{x}', \mathbf{z})$ is measurable. This set is monotone increasing as $n \rightarrow \infty$ to the set of ω for which the alternatives \mathbf{x} and \mathbf{x}' are not tied. By hypothesis, this set has probability one, implying that there exists $\bar{n} = \bar{n}(\mathbf{x}, \mathbf{x}', \mathbf{z}) \in \mathbb{N}_+$ such that we have $\Pr_\omega[\Omega_{\bar{n}}(\mathbf{x}, \mathbf{x}', \mathbf{z})] \geq 1 - \eta/4\kappa$.

2. *There exists a neighborhood where utility remains controlled for different alternatives.* The uniform continuity of $U(\cdot)$ on $\mathcal{X} \times [0, 1]^{d_x} \times \mathcal{Z} \times [0, 1]^{d_z}$ implies that, for every given \bar{n} , there exists $\bar{\delta} = \delta(\mathbf{x}, \mathbf{x}', \mathbf{z}) \in \mathbb{R}_+$ such that in a neighborhood of $\bar{\delta}$, $U(\cdot)$ varies by less than $1/\bar{n}$. The almost certain continuity of $\epsilon(\omega, \mathbf{x})$ and $\nu(\omega, \mathbf{z})$ imply that the set

$$B_m(\mathbf{x}, \mathbf{z}) = \left\{ \omega \in \Omega : \sup_{|\mathbf{x} - \mathbf{x}^*| < 1/m} |\epsilon(\omega, \mathbf{x}) - \epsilon(\omega, \mathbf{x}^*)| + \sup_{|\mathbf{z} - \mathbf{z}^*| < 1/m} |\nu(\omega, \mathbf{z}) - \nu(\omega, \mathbf{z}^*)| \leq \delta(\mathbf{x}, \mathbf{x}', \mathbf{z}) \right\},$$

and the corresponding $B_m(\mathbf{x}', \mathbf{z})$ are monotone increasing as $m \rightarrow \infty$ to limiting sets that occur with probability one. Consequently, there exists $\bar{m} = m(\mathbf{x}, \mathbf{x}', \mathbf{z}) \in \mathbb{N}_+$ such that $\Pr_\omega[B_{\bar{m}}(\mathbf{x}, \mathbf{z})] \geq 1 - \eta/4\kappa$ and $\Pr_\omega[B_{\bar{m}}(\mathbf{x}', \mathbf{z})] \geq 1 - \eta/4\kappa$.

3. *Finite covering.* We have established so far that with probability at least $1 - 3\eta/4\kappa$, $\omega \in \Omega_{\bar{n}}(\mathbf{x}, \mathbf{x}', \mathbf{z}) \cap B_{\bar{m}}(\mathbf{x}, \mathbf{z}) \cap B_{\bar{m}}(\mathbf{x}', \mathbf{z})$ implying that

$$(a) \quad |F(\omega, \mathbf{x}, \mathbf{z}) - F(\omega, \mathbf{x}', \mathbf{z})| \geq 7/\bar{n}$$

(b) For all $(\hat{\mathbf{x}}, \hat{\mathbf{x}}', \hat{\mathbf{z}})$ in an open neighborhood of $(\mathbf{x}, \mathbf{x}', \mathbf{z})$ and of radius $\min\{1/\bar{m}, \bar{\delta}\}$, we have $|F(\omega, \hat{\mathbf{x}}, \hat{\mathbf{z}}) - F(\omega, \mathbf{x}, \mathbf{z})| \leq 1/\bar{n}$ and $|F(\omega, \hat{\mathbf{x}}', \hat{\mathbf{z}}) - F(\omega, \mathbf{x}', \mathbf{z})| \leq 1/\bar{n}$.

These neighborhoods, centered around each $(\mathbf{x}, \mathbf{x}', \mathbf{z})$, cover the compact set $\mathcal{X} \times \mathcal{X} \times \mathcal{Z}$. Consequently, there exists a finite subcovering C . We have established that each point $(\mathbf{x}, \mathbf{x}', \mathbf{z}) \in \mathcal{X} \times \mathcal{X} \times \mathcal{Z}$ falls in some neighborhood of a center $(\hat{\mathbf{x}}, \hat{\mathbf{x}}', \hat{\mathbf{z}}) \in C$ and therefore satisfies

$$\begin{aligned} & |F(\omega, \mathbf{x}, \mathbf{z}) - F(\omega, \mathbf{x}', \mathbf{z})| \\ & \geq |F(\omega, \mathbf{x}, \mathbf{z}) - F(\omega, \hat{\mathbf{x}}, \hat{\mathbf{z}})| - |F(\omega, \hat{\mathbf{x}}, \hat{\mathbf{z}}) - F(\omega, \hat{\mathbf{x}}', \hat{\mathbf{z}})| - |F(\omega, \hat{\mathbf{x}}', \hat{\mathbf{z}}) - F(\omega, \mathbf{x}', \mathbf{z})| \\ & \geq 7/n(\hat{\mathbf{x}}, \hat{\mathbf{x}}', \hat{\mathbf{z}}) - 1/n(\hat{\mathbf{x}}, \hat{\mathbf{x}}', \hat{\mathbf{z}}) - 1/n(\hat{\mathbf{x}}, \hat{\mathbf{x}}', \hat{\mathbf{z}}) \\ & \geq 5/n(\hat{\mathbf{x}}, \hat{\mathbf{x}}', \hat{\mathbf{z}}), \end{aligned}$$

on a set of ω that occurs with probability at least $1 - 3\eta/4\kappa$.

□

B.2. Proof of Proposition 1

We now present the proof of Proposition 1, which proceeds linearly in showing that we can control the errors in the successive layers of approximation of the utility function. Let C denote the finite covering and $\bar{N} = \max\{n(c) : c \in C\}$ that satisfy the properties stated in Lemma EC.1. Let $N \geq \max\{-\log(\eta/4\kappa), \bar{N}\}$ be a sufficiently large integer that will be determined later on. Recall that $\epsilon(\cdot)$ and $\nu(\cdot)$ are random fields over \mathcal{X} and \mathcal{Z} respectively. For analysis purposes, we explicit this randomness. In particular, we introduce a fundamental probability space $(\Omega, \mathcal{W}, \Pr_\omega)$ and denote by $\epsilon(w, \mathbf{x})$ (resp. $\nu(w, \mathbf{z})$) a particular realization of $\epsilon(\mathbf{x})$ (resp. $\nu(\mathbf{z})$). For ease of notation, we let for $(w, \mathbf{x}, \mathbf{z}) \in \Omega \times \mathcal{X} \times \mathcal{Z}$,

$$F(w, \mathbf{x}, \mathbf{z}) = U(\mathbf{x}, \epsilon(w, \mathbf{x}), \mathbf{z}, \nu(w, \mathbf{z})).$$

Recall that for all choice event (\mathbf{z}, A) and $\mathbf{x} \in A$, we have

$$\pi(\mathbf{x}, \mathbf{z}, A) = \Pr_\omega[F(\omega, \mathbf{x}, \mathbf{z}) > F(\omega, \mathbf{x}', \mathbf{z}), \forall \mathbf{x}' \in A \setminus \mathbf{x}].$$

Step 1: Universal approximation and discretization. Feed-forward neural networks are a known class of universal approximators. More specifically, the space of feed-forward neural networks with only one hidden layer and one output unit is dense in $C(X)$, the space of continuous function on X , as long as X is compact and the activation function is continuous, bounded and non-constant (Hornik et al. 1989, Hornik 1991). Consequently, there exists a feed-forward neural network $N_U(\cdot)$ that approximates $U(\cdot)$ on $\mathcal{X} \times [0, 1]^{d_\epsilon} \times \mathcal{Z} \times [0, 1]^{d_\nu}$, i.e. that satisfies $\|U(\cdot) - N_U(\cdot)\|_\infty \leq 1/N$.

By the uniform continuity of $U(\cdot)$, there exists $\delta > 0$, such that for all $(\mathbf{x}, \mathbf{z}) \in \mathcal{X} \times \mathcal{Z}$ and $(\boldsymbol{\epsilon}, \boldsymbol{\epsilon}') \in [0, 1]^{2d_\epsilon}$ and $(\boldsymbol{\nu}, \boldsymbol{\nu}') \in [0, 1]^{2d_\nu}$ such that $\|\boldsymbol{\epsilon} - \boldsymbol{\epsilon}'\|_\infty \leq \delta$ and $\|\boldsymbol{\nu} - \boldsymbol{\nu}'\|_\infty \leq \delta$, we have $|U(\mathbf{x}, \boldsymbol{\epsilon}, \mathbf{z}, \boldsymbol{\nu}) - U(\mathbf{x}, \boldsymbol{\epsilon}', \mathbf{z}, \boldsymbol{\nu}')| \leq 1/N$. For every $\omega \in \Omega$, there exists feed-forward neural networks $N_{\epsilon, \omega}(\mathbf{x})$ and $N_{\nu, \omega}(\mathbf{z})$ that approximate $\boldsymbol{\epsilon}(\omega, \mathbf{x})$ and $\boldsymbol{\nu}(\omega, \mathbf{z})$ on \mathcal{X} and \mathcal{Z} respectively, i.e., $\|\boldsymbol{\epsilon}(\omega, \mathbf{x}) - N_{\epsilon, \omega}(\mathbf{x})\|_\infty \leq \delta$ for all $\mathbf{x} \in \mathcal{X}$ and $\|\boldsymbol{\nu}(\omega, \mathbf{z}) - N_{\nu, \omega}(\mathbf{z})\|_\infty \leq \delta$ for all $\mathbf{z} \in \mathcal{Z}$. Consequently, for all $\mathbf{x} \in \mathcal{X}$, $\omega \in \Omega$ and $\mathbf{z} \in \mathcal{Z}$, we have

$$|U(\mathbf{x}, \boldsymbol{\epsilon}(\omega, \mathbf{x}), \mathbf{z}, \boldsymbol{\nu}(\omega, \mathbf{z})) - N_U(\mathbf{x}, N_{\epsilon, \omega}(\mathbf{x}), \mathbf{z}, N_{\nu, \omega}(\mathbf{z}))| \leq \frac{2}{N}, \quad (\text{EC.1})$$

since $|N_U(\mathbf{x}, N_{\epsilon, \omega}(\mathbf{x}), \mathbf{z}, N_{\nu, \omega}(\mathbf{z})) - U(\mathbf{x}, N_{\epsilon, \omega}(\mathbf{x}), \mathbf{z}, N_{\nu, \omega}(\mathbf{z}))| \leq 1/N$ in light of the uniform approximation of $U(\cdot)$ by $N_U(\cdot)$ and $|U(\mathbf{x}, N_{\epsilon, \omega}(\mathbf{x}), \mathbf{z}, N_{\nu, \omega}(\mathbf{z})) - U(\mathbf{x}, \boldsymbol{\epsilon}(\omega, \mathbf{x}), \mathbf{z}, \boldsymbol{\nu}(\omega, \mathbf{z}))| \leq 1/N$ due to the uniform continuity of $U(\cdot)$.

Step 2: Adding noise. Throughout the remainder of the proof, we fix a choice set A , an alternative $\mathbf{x} \in A$, and customer attributes $\mathbf{z} \in \mathcal{Z}$. For each $\mathbf{x} \in A$, we define a utility $F^1(\cdot)$ as follows:

$$F^1(\omega, \delta_{\mathbf{x}}, \mathbf{x}, \mathbf{z}) = N_U(\mathbf{x}, N_{\epsilon, \omega}(\mathbf{x}), \mathbf{z}, N_{\nu, \omega}(\mathbf{z})) + \frac{\delta_{\mathbf{x}}}{N^2}, \quad (\text{EC.2})$$

where $\boldsymbol{\delta} = \{\delta_{\mathbf{x}}\}_{\mathbf{x} \in A}$ is a sequence i.i.d. random variables following a standard Gumbel distribution. Let

$$\pi^1(\mathbf{x}, \mathbf{z}, A) = \Pr_{\omega, \boldsymbol{\delta}}[F^1(\omega, \delta_{\mathbf{x}}, \mathbf{x}, \mathbf{z}) > F^1(\omega, \delta_{\mathbf{x}'}, \mathbf{x}', \mathbf{z}), \forall \mathbf{x}' \in A \setminus \{\mathbf{x}\}],$$

be the choice probability associated with the utility $F^1(\cdot)$. For all $\mathbf{x}' \in A \setminus \{\mathbf{x}\}$, let

$$\Omega_{\mathbf{x}, \mathbf{x}'}^1 = \{\omega \in \Omega, (\delta_{\mathbf{x}}, \delta_{\mathbf{x}'}) \in \mathbb{R}^2 : (F(\omega, \mathbf{x}, \mathbf{z}) - F(\omega, \mathbf{x}', \mathbf{z})) \times (F^1(\omega, \delta_{\mathbf{x}}, \mathbf{x}, \mathbf{z}) - F^1(\omega, \delta_{\mathbf{x}'}, \mathbf{x}', \mathbf{z})) < 0\}$$

be the collection of realisations for which the preferences over alternatives \mathbf{x} and \mathbf{x}' are reversed when using $F^1(\cdot)$ instead of $F(\cdot)$. Note that

$$|\pi(\mathbf{x}, \mathbf{z}, A) - \pi^1(\mathbf{x}, \mathbf{z}, A)| \leq \Pr \left[\bigcup_{\mathbf{x}' \in A \setminus \{\mathbf{x}\}} \Omega_{\mathbf{x}, \mathbf{x}'}^1 \right] \leq \sum_{\mathbf{x}' \in A \setminus \{\mathbf{x}\}} \Pr [\Omega_{\mathbf{x}, \mathbf{x}'}^1] \leq \kappa \cdot \Pr [\Omega_{\mathbf{x}, \mathbf{x}'}^1],$$

where the first inequality holds follows by noting that for $F^1(\cdot)$ to designate \mathbf{x} as the the highest-utility alternative in the choice set A , while $F(\cdot)$ designates a different alternative \mathbf{x}' in the choice set A , there needs to be a reversal of preferences between \mathbf{x} and \mathbf{x}' . The second inequality follows from the union bound. Without loss of generality, consider $\omega \in \Omega$ and $(\delta_{\mathbf{x}}, \delta_{\mathbf{x}'}) \in \mathbb{R}^2$ such that

$$F(\omega, \mathbf{x}, \mathbf{z}) > F(\omega, \mathbf{x}', \mathbf{z}) \text{ and } F^1(\omega, \delta_{\mathbf{x}}, \mathbf{x}, \mathbf{z}) < F^1(\omega, \delta_{\mathbf{x}'}, \mathbf{x}', \mathbf{z}).$$

If $|F(\omega, \mathbf{x}, \mathbf{z}) - F(\omega, \mathbf{x}', \mathbf{z})| > 5/N$, then

$$\begin{aligned} 0 &> F^1(\omega, \delta_{\mathbf{x}}, \mathbf{x}, \mathbf{z}) - F^1(\omega, \delta_{\mathbf{x}'}, \mathbf{x}', \mathbf{z}) \\ &= N_U(\mathbf{x}, N_{\epsilon, \omega}(\mathbf{x}), \mathbf{z}, N_{\nu, \omega}(\mathbf{z})) - N_U(\mathbf{x}', N_{\epsilon, \omega}(\mathbf{x}'), \mathbf{z}, N_{\nu, \omega}(\mathbf{z})) + (\delta_{\mathbf{x}} - \delta_{\mathbf{x}'}) \\ &> F(\omega, \mathbf{x}, \mathbf{z}) - F(\omega, \mathbf{x}', \mathbf{z}) - 4/N + (\delta_{\mathbf{x}} - \delta_{\mathbf{x}'})/N^2 \\ &\geq 1/N + (\delta_{\mathbf{x}} - \delta_{\mathbf{x}'})/N^2, \end{aligned}$$

where the second inequality holds by Equation (EC.1). Consequently, $\delta_{\mathbf{x}} - \delta_{\mathbf{x}'} \leq -N$. Under the Gumbel assumption, we have for $N \geq -\log(\eta/4\kappa)$, $\Pr_{\delta}[\delta_{\mathbf{x}} - \delta_{\mathbf{x}'} \leq -N] < \eta/4\kappa$. From Lemma EC.1, the probability that $|F(\omega, \mathbf{x}, \mathbf{z}) - F(\omega, \mathbf{x}', \mathbf{z})| \leq 5/N$ is at most $3\eta/4\kappa$. Consequently, $\Pr[\Omega_{\mathbf{x}, \mathbf{x}'}^1] \leq \eta/\kappa$ which in turn implies that

$$|\pi(\mathbf{x}, \mathbf{z}, A) - \pi^1(\mathbf{x}, \mathbf{z}, A)| \leq \eta. \quad (\text{EC.3})$$

Step 3: Sampling error. For purposes of analysis, we need to refine the finite covering constructed in Lemma EC.1. In particular, for every $\mathbf{x} \in \mathcal{X}$, $\mathbf{z} \in \mathcal{Z}$, $\omega \in \Omega$ and $\delta \in \mathbb{R}$, we define the mapping $\bar{F}^1(\omega, \mathbf{x}, \mathbf{z}) = N_U(\mathbf{x}, N_{\epsilon, \omega}(\mathbf{x}), \mathbf{z}, N_{\nu, \omega}(\mathbf{z}))$. Next, we construct a finite covering that is mutually adapted to F and \bar{F}^1 in the sense of Lemma EC.1. Specifically, there exists a finite covering $(B(c, \delta^+(c)))_{c \in C^+}$ with centers $C^+ \subseteq \mathcal{X}^2 \times \mathcal{Z}$, radii $(\delta^+(c))_{c \in C^+}$, and integers $(n^+(c))_{c \in C^+}$ such that, given a fixed $c = (\tilde{\mathbf{x}}, \tilde{\mathbf{x}'}, \tilde{\mathbf{z}}) \in C^+$, with probability at least $1 - 3\eta/4\kappa$, we have for all $(\mathbf{x}, \mathbf{x}', \mathbf{z}) \in \mathcal{X}^2 \times \mathcal{Z}$ in the neighborhood of $(\tilde{\mathbf{x}}, \tilde{\mathbf{x}'}, \tilde{\mathbf{z}})$ that:

1. $|\bar{F}^1(\omega, \mathbf{x}, \mathbf{z}) - \bar{F}^1(\omega, \tilde{\mathbf{x}}, \tilde{\mathbf{z}})| \leq 1/n^+(c)$ and $|F(\omega, \mathbf{x}, \mathbf{z}) - F(\omega, \tilde{\mathbf{x}}, \tilde{\mathbf{z}})| \leq 1/n^+(c)$,
2. $|\bar{F}^1(\omega, \mathbf{x}', \mathbf{z}) - \bar{F}^1(\omega, \tilde{\mathbf{x}'}, \tilde{\mathbf{z}})| \leq 1/n^+(c)$ and $|F(\omega, \mathbf{x}', \mathbf{z}) - F(\omega, \tilde{\mathbf{x}'}, \tilde{\mathbf{z}})| \leq 1/n^+(c)$,
3. $|\bar{F}^1(\omega, \tilde{\mathbf{x}}, \tilde{\mathbf{z}}) - \bar{F}^1(\omega, \tilde{\mathbf{x}'}, \tilde{\mathbf{z}})| \geq 5/n^+(c)$ and $|F(\omega, \tilde{\mathbf{x}}, \tilde{\mathbf{z}}) - F(\omega, \tilde{\mathbf{x}'}, \tilde{\mathbf{z}})| \geq 5/n^+(c)$.

Consequently, we set the precise value of N as $N = \max\{-\log(\eta/8\kappa), \bar{N}, \max\{n^+(c) : c \in C^+\}\}$. Next, we construct a mapping from any choice set A to $\hat{A} = \{\hat{\mathbf{x}}_1, \dots, \hat{\mathbf{x}}_K\}$, where each alternative $\mathbf{x} \in A$ is replaced by a fixed element $\hat{\mathbf{x}}$ of $\bigcap_{c \in C^+(\mathbf{x})} \{y_1 : \mathbf{y} \in B(c, \delta^+(c))\}$ where $C^+(\mathbf{x})$ denotes all the centers $c \in C^+$ such that $(\mathbf{x}, c_2, c_3) \in B(c, \delta^+(c))$. Note that the latter intersection of open balls is non-empty since it contains \mathbf{x} . Similarly, each $\mathbf{z} \in \mathcal{Z}$ is mapped to a fixed element $\hat{\mathbf{z}}$ of $\bigcap_{c \in C^+(\mathbf{z})} \{y_3 : \mathbf{y} \in B(c, \delta^+(c))\}$ where $C^+(\mathbf{z})$ denotes all the centers $c \in C^+$ such that $(c_1, c_2, \mathbf{z}) \in$

$B(c, \delta^+(c))$. Let \mathcal{E} be the collection of all choice events $(\hat{\mathbf{x}}, \hat{\mathbf{z}}, \hat{A})$ generated by our mapping. Clearly, since the covering is finite, \mathcal{E} is also finite. We proceed to establish the following claim, whose proof is presented in Appendix B.3.

CLAIM EC.1. *For every choice event $(\mathbf{x}, \mathbf{A}, \mathbf{z}) \in \mathcal{X}^{\kappa+1} \times \mathcal{Z}$, we have*

$$|\pi(\mathbf{x}, \mathbf{z}, A) - \pi(\hat{\mathbf{x}}, \hat{\mathbf{z}}, \hat{A})| \leq \eta \text{ and } |\pi^1(\mathbf{x}, \mathbf{z}, A) - \pi^1(\hat{\mathbf{x}}, \hat{\mathbf{z}}, \hat{A})| \leq \eta . \quad (\text{EC.4})$$

The final piece of our proof is to construct a sample average approximation of $\pi^1(\cdot)$ with respect to ω . Let $\hat{\omega} = (\hat{\omega}_1, \dots, \hat{\omega}_K)$ be K i.i.d. samples based on the probabilistic space $(\Omega, \mathcal{W}, \text{Pr}_\omega)$ where the precise value of K is specified later on. We define the *sampled utility* $F^{2,k}(\delta_{\mathbf{x}}, \mathbf{x}, \mathbf{z})$ as follows:

$$F^{2,k}(\delta_{\mathbf{x}}, \mathbf{x}, \mathbf{z}) = F^1(\hat{\omega}_k, \delta_{\mathbf{x}}, \mathbf{x}, \mathbf{z}) = N_U(\mathbf{x}, N_{\epsilon, \hat{\omega}_k}(\mathbf{x}), \mathbf{z}, N_{\nu, \hat{\omega}_k}(\mathbf{z})) + \frac{\delta_{\mathbf{x}}}{N^2} . \quad (\text{EC.5})$$

By Equation (EC.2), $F^{2,k}(\delta_{\mathbf{x}}, \mathbf{x}, \mathbf{z})$ can be interpreted as the realisation of $F^1(\omega, \delta_{\mathbf{x}}, \mathbf{x}, \mathbf{z})$ with respect to the sample $\hat{\omega}_k$. However, it is worth observing that $F^{2,k}(\delta_{\mathbf{x}}, \mathbf{x}, \mathbf{z})$ is itself a random variable due to the noise term $\delta_{\mathbf{x}}$. Finally, we let $\pi^2(\mathbf{x}, \mathbf{z}, A)$ be the sample mean estimator of the choice probabilities with respect to $F^{2,1}, \dots, F^{2,K}$, i.e.

$$\pi^2(\mathbf{x}, \mathbf{z}, A) = \frac{1}{K} \cdot \sum_{k=1}^K \text{Pr}_\delta [F^{2,k}(\delta_{\mathbf{x}}, \mathbf{x}, \mathbf{z}) > F^{2,k}(\delta_{\mathbf{x}'}, \mathbf{x}', \mathbf{z}), \forall \mathbf{x}' \in A \setminus \{\mathbf{x}\}] . \quad (\text{EC.6})$$

By Equations (EC.5) and (EC.6), it is clear that the choice model $\pi^2(\cdot)$ can be represented by an instance of the RUMnet architecture. Hence, we denote by $N(\hat{\omega}) \in \mathcal{N}^d(K, \Theta_M^{\ell, w})$ the RUMnet architecture such that $\pi^2(\cdot) = \pi_{N(\hat{\omega})}^{\text{RUMnet}}(\cdot)$.

Next, we analyse the differences between the choice models $\pi^1(\cdot)$ and its sample mean approximation $\pi_{N(\hat{\omega})}^{\text{RUMnet}}(\cdot)$. First, we establish a property analogous to Claim EC.1 with respect to $\pi^2(\cdot)$. The proof is provided in Appendix B.4

CLAIM EC.2. *For any $K \geq \frac{\kappa^2 \log(4|\mathcal{E}|)}{2 \cdot \eta^2}$, with probability at least $3/4$ with respect to $\hat{\omega}$, for all choice events $(\mathbf{x}, \mathbf{A}, \mathbf{z}) \in \mathcal{X}^{\kappa+1} \times \mathcal{Z}$, we have*

$$|\pi_{N(\hat{\omega})}^{\text{RUMnet}}(\mathbf{x}, \mathbf{z}, A) - \pi_{N(\hat{\omega})}^{\text{RUMnet}}(\hat{\mathbf{x}}, \hat{\mathbf{z}}, \hat{A})| \leq 2\eta .$$

Next, we observe that, for all $K \geq \frac{\kappa^2 \log(4|\mathcal{E}|)}{2 \cdot \eta^2}$,

$$\begin{aligned} & \text{Pr}_{\hat{\omega}} \left[\max_{((\mathbf{x}, \hat{\mathbf{z}}), \hat{A}) \in \mathcal{E}} \left| \pi^1(\hat{\mathbf{x}}, \hat{\mathbf{z}}, \hat{A}) - \pi_{N(\hat{\omega})}^{\text{RUMnet}}(\hat{\mathbf{x}}, \hat{\mathbf{z}}, \hat{A}) \right| > \eta \right] \\ & \leq \sum_{(\mathbf{x}, \hat{\mathbf{z}}, \hat{A}) \in \mathcal{E}} \text{Pr}_{\hat{\omega}} \left[\left| \pi^1(\hat{\mathbf{x}}, \hat{\mathbf{z}}, \hat{A}) - \pi_{N(\hat{\omega})}^{\text{RUMnet}}(\hat{\mathbf{x}}, \hat{\mathbf{z}}, \hat{A}) \right| > \eta \right] \\ & \leq \sum_{(\mathbf{x}, \hat{\mathbf{z}}, \hat{A}) \in \mathcal{E}} 2 \cdot e^{-2 \cdot \eta^2 \frac{\log(8|\mathcal{P}|)}{2 \cdot \eta^2}} \\ & \leq \frac{1}{2} , \end{aligned} \quad (\text{EC.7})$$

where the first inequality follows from the union bound and the second inequality from Hoeffding's inequality. Fix $K = \lceil \frac{\kappa^2 \log(4|\mathcal{E}|)}{2\eta^2} \rceil$. By the union bound over Inequality (EC.7) and Claim EC.2, there exists a realization $\hat{\omega}^*$ of $\hat{\omega}$ such that, for all $(\hat{\mathbf{x}}, \hat{\mathbf{z}}, \hat{A}) \in \mathcal{E}$, we have

$$\left| \pi^1(\hat{\mathbf{x}}, \hat{\mathbf{z}}, \hat{A}) - \pi_{N(\hat{\omega}^*)}^{\text{RUMnet}}(\hat{\mathbf{x}}, \hat{\mathbf{z}}, \hat{A}) \right| \leq \eta . \quad (\text{EC.8})$$

and for all choice events $(\mathbf{x}, \mathbf{A}, \mathbf{z}) \in \mathcal{X}^{\kappa+1} \times \mathcal{Z}$, we have

$$\left| \pi_{N(\hat{\omega}^*)}^{\text{RUMnet}}(\mathbf{x}, \mathbf{z}, A) - \pi_{N(\hat{\omega}^*)}^{\text{RUMnet}}(\hat{\mathbf{x}}, \hat{\mathbf{z}}, \hat{A}) \right| \leq 2\eta . \quad (\text{EC.9})$$

Putting Claim EC.1, Inequalities (EC.3), (EC.8) and (EC.9) together, we have

$$\begin{aligned} & \left| \pi(\mathbf{x}, \mathbf{z}, A) - \pi_{N(\hat{\omega}^*)}^{\text{RUMnet}}(\mathbf{x}, \mathbf{z}, A) \right| \\ & \leq \left| \pi(\mathbf{x}, \mathbf{z}, A) - \pi(\hat{\mathbf{x}}, \hat{\mathbf{z}}, \hat{A}) \right| + \left| \pi(\hat{\mathbf{x}}, \hat{\mathbf{z}}, \hat{A}) - \pi^1(\hat{\mathbf{x}}, \hat{\mathbf{z}}, \hat{A}) \right| + \left| \pi^1(\hat{\mathbf{x}}, \hat{\mathbf{z}}, \hat{A}) - \pi_{N(\hat{\omega}^*)}^{\text{RUMnet}}(\hat{\mathbf{x}}, \hat{\mathbf{z}}, \hat{A}) \right| \\ & \quad + \left| \pi_{N(\hat{\omega}^*)}^{\text{RUMnet}}(\hat{\mathbf{x}}, \hat{\mathbf{z}}, \hat{A}) - \pi_{N(\hat{\omega}^*)}^{\text{RUMnet}}(\mathbf{x}, \mathbf{z}, A) \right| \\ & \leq 5\eta , \end{aligned}$$

which yields the desired result. \square

B.3. Proof of Claim EC.1

We establish the desired inequality for the choice model $\pi^1(\cdot)$ since the case of $\pi(\cdot)$ proceeds from an identical reasoning. As in Step 2, we define $\Omega_{\mathbf{x}, \mathbf{x}'}$ for every $\mathbf{x}' \in A \setminus \{\mathbf{x}\}$ as the event where customer \mathbf{z} 's preferences over $(\mathbf{x}, \mathbf{x}')$ are reversed compared to customer $\hat{\mathbf{z}}$'s preferences over $(\hat{\mathbf{x}}, \hat{\mathbf{x}'})$ with respect to the random utility function $F^1(\omega, \delta, \cdot, \cdot)$. By the union bound, we have

$$\left| \pi(\mathbf{x}, \mathbf{z}, A) - \pi(\hat{\mathbf{x}}, \hat{\mathbf{z}}, \hat{A}) \right| \leq \sum_{\mathbf{x}' \in A \setminus \{\mathbf{x}\}} \Pr[\Omega_{\mathbf{x}, \mathbf{x}'}] \leq \kappa \cdot \max_{\mathbf{x}' \in A \setminus \{\mathbf{x}\}} \Pr[\Omega_{\mathbf{x}, \mathbf{x}'}] . \quad (\text{EC.10})$$

Without loss of generality, fix $\mathbf{x}, \mathbf{x}' \in A^2$ and consider $\omega \in \Omega$ and $(\delta_{\mathbf{x}}, \delta_{\mathbf{x}'}) \in \mathbb{R}^2$ such that

$$F^1(\omega, \delta_{\mathbf{x}}, \mathbf{x}, \mathbf{z}) > F^1(\omega, \delta_{\mathbf{x}'}, \mathbf{x}', \mathbf{z}) \text{ and } F^1(\omega, \delta_{\hat{\mathbf{x}}}, \hat{\mathbf{x}}, \hat{\mathbf{z}}) < F^1(\omega, \delta_{\hat{\mathbf{x}'}} , \hat{\mathbf{x}}', \hat{\mathbf{z}}).$$

Now, let $c = (\tilde{\mathbf{x}}, \tilde{\mathbf{x}'}, \tilde{\mathbf{z}}) \in C^+$ be the center of a neighborhood that contains $(\mathbf{x}, \mathbf{x}', \mathbf{z})$. By construction of our mapping, this neighborhood necessarily contains $(\hat{\mathbf{x}}, \hat{\mathbf{x}'}, \hat{\mathbf{z}})$ based on the coordinate-wise inequalities $\delta^+(c) \geq \max\{|\hat{\mathbf{x}} - \mathbf{x}|, |\hat{\mathbf{x}}' - \mathbf{x}'|, |\hat{\mathbf{z}} - \mathbf{z}|\}$, which imply that $(\hat{\mathbf{x}}, \hat{\mathbf{x}'}, \hat{\mathbf{z}}) \in B(c, \delta^+(c))$. In what follows, suppose that ω satisfies properties 1-3. We note that this event occurs with probability at least $1 - 3\eta/4\kappa$. Due to properties 1-2, we have

$$\begin{aligned} 0 & > F^1(\omega, \delta_{\hat{\mathbf{x}}}, \hat{\mathbf{x}}, \hat{\mathbf{z}}) - F^1(\omega, \delta_{\hat{\mathbf{x}'}} , \hat{\mathbf{x}}', \hat{\mathbf{z}}) \\ & \geq \bar{F}^1(\omega, \tilde{\mathbf{x}}, \tilde{\mathbf{z}}) - \bar{F}^1(\omega, \tilde{\mathbf{x}}', \tilde{\mathbf{z}}) - |\bar{F}^1(\omega, \hat{\mathbf{x}}, \hat{\mathbf{z}}) - \bar{F}^1(\omega, \tilde{\mathbf{x}}, \tilde{\mathbf{z}})| - |\bar{F}^1(\omega, \hat{\mathbf{x}}', \hat{\mathbf{z}}) - \bar{F}^1(\omega, \tilde{\mathbf{x}}', \tilde{\mathbf{z}})| + (\delta_{\hat{\mathbf{x}}} - \delta_{\hat{\mathbf{x}'}})/N^2 \\ & \geq \bar{F}^1(\omega, \tilde{\mathbf{x}}, \tilde{\mathbf{z}}) - \bar{F}^1(\omega, \tilde{\mathbf{x}}', \tilde{\mathbf{z}}) - 2/n^+(c) + (\delta_{\hat{\mathbf{x}}} - \delta_{\hat{\mathbf{x}'}})/N^2 , \end{aligned}$$

and

$$\begin{aligned}
0 &< F^1(\omega, \delta_{\mathbf{x}}, \mathbf{x}, \mathbf{z}) - F^1(\omega, \delta_{\mathbf{x}'}, \mathbf{x}', \mathbf{z}) \\
&\leq \bar{F}^1(\omega, \tilde{\mathbf{x}}, \tilde{\mathbf{z}}) - \bar{F}^1(\omega, \tilde{\mathbf{x}}', \tilde{\mathbf{z}}) + |\bar{F}^1(\omega, \mathbf{x}, \mathbf{z}) - \bar{F}^1(\omega, \tilde{\mathbf{x}}, \tilde{\mathbf{z}})| + |\bar{F}^1(\omega, \mathbf{x}', \mathbf{z}) - \bar{F}^1(\omega, \tilde{\mathbf{x}}', \tilde{\mathbf{z}})| + (\delta_{\mathbf{x}} - \delta_{\mathbf{x}'})/N^2 \\
&\leq \bar{F}^1(\omega, \tilde{\mathbf{x}}, \tilde{\mathbf{z}}) - \bar{F}^1(\omega, \tilde{\mathbf{x}}', \tilde{\mathbf{z}}) + 2/n^+(c) + (\delta_{\mathbf{x}} - \delta_{\mathbf{x}'})/N^2 .
\end{aligned}$$

Combining these inequalities with property 3, we infer that either $\delta_{\hat{\mathbf{x}}} - \delta_{\hat{\mathbf{x}}}' \leq -3\frac{N^2}{n^+(c)} \leq -3N$ or $\delta_{\mathbf{x}} - \delta_{\mathbf{x}}' \geq 3\frac{N^2}{n^+(c)} \geq 3N$. Since $N \geq -\log(\frac{\eta}{8\kappa})$ and δ is a collection of i.i.d. Gumbel random variables, each of these events occurs with probability at most $\frac{\eta}{8\kappa}$. By the union bound, we derive the upper bound on reversal probabilities:

$$\Pr[\Omega_{\mathbf{x}, \mathbf{x}'}] \leq \frac{3\eta}{4\kappa} + 2\frac{\eta}{8\kappa} = \frac{\eta}{\kappa} .$$

The desired inequality immediately follows by plugging the above inequality into (EC.10).

B.4. Proof of Claim EC.2

Fix a choice event $(\mathbf{x}, \mathbf{A}, \mathbf{z}) \in \mathcal{X}^{\kappa+1} \times \mathcal{Z}$. Similarly to the proof of Claim EC.1, for each $\mathbf{x}' \in A \setminus \{\mathbf{x}'\}$ and $k \in [K]$, we develop an upper bound on the probability of a preference reversal conditional to the sample $\hat{\omega}$. Specifically, the preference reversal event $\Omega_{\mathbf{x}, \mathbf{x}', \mathbf{z}}^k$ occurs when customer \mathbf{z} 's preferences over $(\mathbf{x}, \mathbf{x}')$ are reversed compared to customer $\hat{\mathbf{z}}$'s preferences over $(\hat{\mathbf{x}}, \hat{\mathbf{x}}')$ with respect to the k -th sampled random utility function $F^{2,k}(\delta, \cdot, \cdot) = F^1(\hat{\omega}_k, \delta, \cdot, \cdot)$. Let $G_{\mathbf{x}, \mathbf{x}', \mathbf{z}}^k$ denote the event for which $\hat{\omega}_k$ satisfies properties 1-3 with respect to $(\tilde{\mathbf{x}}, \tilde{\mathbf{x}}', \tilde{\mathbf{z}})$. Since $(\hat{\mathbf{x}}, \hat{\mathbf{x}}', \hat{\mathbf{z}})$ is contained in the same neighborhood of the covering, we have $G_{\mathbf{x}, \mathbf{x}', \mathbf{z}}^k = G_{\hat{\mathbf{x}}, \hat{\mathbf{x}}', \hat{\mathbf{z}}}^k$. Now, a close examination of the proof of Claim EC.1 reveals that, conditional on $G_{\hat{\mathbf{x}}, \hat{\mathbf{x}}', \hat{\mathbf{z}}}^k$, the preference reversal occurs with probability at most $\frac{\eta}{4\kappa}$. It follows that:

$$\begin{aligned}
&|\pi_{N(\hat{\omega})}^{\text{RUMnet}}(\mathbf{x}, \mathbf{z}, A) - \pi_{N(\hat{\omega})}^{\text{RUMnet}}(\hat{\mathbf{x}}, \hat{\mathbf{z}}, \hat{A})| \\
&\leq \frac{1}{K} \cdot \sum_{k=1}^K \Pr \left[\bigcup_{\mathbf{x}' \in A \setminus \{\mathbf{x}\}} \Omega_{\mathbf{x}, \mathbf{x}', \mathbf{z}}^k \middle| \hat{\omega} \right] \\
&\leq \frac{1}{K} \cdot \sum_{k=1}^K \sum_{\mathbf{x}' \in A \setminus \{\mathbf{x}\}} \Pr_{\delta} [\Omega_{\mathbf{x}, \mathbf{x}', \mathbf{z}}^k | \hat{\omega}_k] \\
&\leq \frac{1}{K} \cdot \sum_{k=1}^K \sum_{\mathbf{x}' \in A \setminus \{\mathbf{x}\}} (\mathbb{I}[\hat{\omega}_k \notin G_{\hat{\mathbf{x}}, \hat{\mathbf{x}}', \hat{\mathbf{z}}}^k] + \Pr [\Omega_{\mathbf{x}, \mathbf{x}', \mathbf{z}}^k | G_{\hat{\mathbf{x}}, \hat{\mathbf{x}}', \hat{\mathbf{z}}}^k] \cdot \mathbb{I}[\hat{\omega}_k \in G_{\hat{\mathbf{x}}, \hat{\mathbf{x}}', \hat{\mathbf{z}}}^k]) \\
&\leq \frac{1}{K} \cdot \sum_{k=1}^K \sum_{\mathbf{x}' \in A \setminus \{\mathbf{x}\}} \left(\mathbb{I}[\hat{\omega}_k \notin G_{\hat{\mathbf{x}}, \hat{\mathbf{x}}', \hat{\mathbf{z}}}^k] + \frac{\eta}{4\kappa} \cdot \mathbb{I}[\hat{\omega}_k \in G_{\hat{\mathbf{x}}, \hat{\mathbf{x}}', \hat{\mathbf{z}}}^k] \right) \\
&\leq \frac{\eta}{4} + \sum_{\mathbf{x}' \in A \setminus \{\mathbf{x}\}} \frac{1}{K} \cdot \sum_{k=1}^K \mathbb{I}[\hat{\omega}_k \notin G_{\hat{\mathbf{x}}, \hat{\mathbf{x}}', \hat{\mathbf{z}}}^k] ,
\end{aligned}$$

where the first inequality holds since, absent a preference reversal over one pair $(\mathbf{x}, \mathbf{x}')$, our RUM-net model identifies the same highest-utility alternative in the assortments A and \hat{A} . The second inequality proceed from the union bound. The next inequality follows from the formula of conditional expectations. The fourth inequality is direct consequence of our upper bound derived from the proof of Claim EC.1. Now, we invoke Hoeffding's inequality so that, for every $\hat{\mathbf{x}}' \in \hat{A}$, we have

$$\Pr_{\hat{\omega}} \left[\frac{1}{K} \sum_{k=1}^K \mathbb{I}[\hat{\omega}_k \notin G_{\hat{\mathbf{x}}, \hat{\mathbf{x}}', \hat{\mathbf{z}}}^k] - \frac{3\eta}{4\kappa} > \frac{\eta}{\kappa} \right] \leq e^{-2\frac{\eta^2}{\kappa^2}K},$$

where we note that $\mathbb{E}_{\hat{\omega}}[\frac{1}{K} \sum_{k=1}^K \mathbb{I}[\hat{\omega}_k \notin G_{\hat{\mathbf{x}}, \hat{\mathbf{x}}', \hat{\mathbf{z}}}^k]] = \Pr[\hat{\omega}_k \notin G_{\hat{\mathbf{x}}, \hat{\mathbf{x}}', \hat{\mathbf{z}}}^k] \leq \frac{3\eta}{4\kappa}$ based on the construction of our covering. By the union bound, we have

$$\begin{aligned} & \Pr_{\hat{\omega}} \left[\exists (\mathbf{x}, \mathbf{A}, \mathbf{z}) \in \mathcal{X}^{\kappa+1} \times \mathcal{Z} \text{ s.t. } |\pi_{N(\hat{\omega})}^{\text{RUMnet}}(\mathbf{x}, \mathbf{z}, A) - \pi_{N(\hat{\omega})}^{\text{RUMnet}}(\hat{\mathbf{x}}, \hat{\mathbf{z}}, \hat{A})| > 2\eta \right] \\ & \leq |\mathcal{E}| \cdot e^{-2\frac{\eta^2}{\kappa^2}K} \\ & \leq \frac{1}{4}. \end{aligned}$$

where the first inequality holds since the number of distinct vectors $(\hat{\mathbf{x}}, \hat{\mathbf{x}}', \hat{\mathbf{z}})$ is upper bounded by $|\mathcal{E}|$ and the next inequality immediately follows from the definition of K .

Appendix C: Proofs of Section 4

C.1. Proof of Proposition 3

Let \mathcal{H} be a hypothesis class, \mathcal{Z} be a collection of data observations endowed with a distribution \mathcal{D} , and $\ell(\cdot)$ be a loss function with respect to \mathcal{H} and \mathcal{Z} . For every hypothesis $h \in \mathcal{H}$, training sample $S = \{\mathbf{z}_1, \dots, \mathbf{z}_T\}$, and loss function $\ell(\cdot)$, we define the empirical error as

$$L_S(h) = \frac{1}{T} \cdot \sum_{t=1}^T \ell(h(\mathbf{z}_t)),$$

and the associated true error

$$L_{\mathcal{D}}^{\text{true}}(h) = \mathbb{E}_{S' \sim \mathcal{D}^n} [L_{S'}(h)].$$

For a given training sample S , let h_S^{ERM} be the hypothesis that minimizes the empirical error $L_S(h)$ over all $h \in \mathcal{H}$. We begin by invoking a classical result to bound the generalization based on the Rademacher complexity; e.g., see [Shalev-Shwartz and Ben-David \(2014\)](#), [Koltchinskii and Panchenko \(2000\)](#), [Bartlett and Mendelson \(2002\)](#). Recall that the Rademacher complexity for a set of vectors $A \subseteq \mathbb{R}^m$ is

$$R(A) = \frac{1}{m} \cdot \mathbb{E}_{\boldsymbol{\sigma}} \left[\sup_{a \in A} \sum_{i=1}^m \sigma_i a_i \right],$$

where $\boldsymbol{\sigma} = (\sigma_1, \dots, \sigma_m)$ is a sequence of independent random variables with $\Pr[\sigma_i = 1] = \Pr[\sigma_i = -1] = \frac{1}{2}$.

THEOREM EC.1 (Shalev-Swartz and Ben-David (2014, Thm. 26.5)). *Suppose that for every hypothesis $h \in \mathcal{H}$ and observation $\mathbf{z} \in \mathcal{Z}$, we have $|\ell(h(\mathbf{z}))| \leq c$ for some $c \geq 0$. Then, with probability of at least $(1 - \delta)$ with regards to the data sample $S \sim \mathcal{D}^T$, we have*

$$L_{\mathcal{D}}^{\text{true}}(h_S^{\text{ERM}}) \leq L_S(h_S^{\text{ERM}}) + 2R(\ell \circ \mathcal{H} \circ S) + 4c\sqrt{\frac{2\ln(4/\delta)}{T}},$$

where $\ell \circ \mathcal{H} \circ S = \{(\ell(h(\mathbf{z}_1)), \dots, \ell(h(\mathbf{z}_T))) : h \in \mathcal{H}\}$.

This type of bound is often referred to as a data-dependent bound since the bound depends on the specific training set S . It therefore suffices to bound the Rademacher complexity of the RUMnet class $\mathcal{N}^d(K, \Theta_M^{\ell, w})$ composed with out data generative process and the negative log-likelihood loss function. Proposition 3 immediately follows from Lemma EC.2 below.

LEMMA EC.2. *Let $\ell(\cdot)$ be the negative log-likelihood loss function, $\mathcal{H}_{\text{RUMnet}}$ be the class of RUMnet class and $S = ((\mathbf{z}_1, A_1), \dots, (\mathbf{z}_T, A_T))$ be a training sample. Then, there exists a constant $c_1 > 0$ such that*

$$R(\ell \circ \mathcal{H}_{\text{RUMnet}} \circ S) \leq c_1 \cdot \frac{\kappa\sqrt{\kappa}}{\sqrt{T}} \cdot e^{2w \cdot M} M^\ell.$$

The remainder of this section established Lemma EC.2. The proof follows by plugging together various notions of Rademacher calculus. For this purpose, we first invoke a number of auxiliary results established in the previous literature. The following claim can be found in Wolf (2018, Corollary 2.4).

LEMMA EC.3 (Rademacher complexity of neural networks). *Let $a, b > 0$. Fix a neural network architecture with $\ell \geq 1$ layers and assume that (i) the activation function σ is 1-Lipschitz and anti-symmetric ($\sigma(-x) = -\sigma(x)$), and (ii) the weight vector w and bias v for every node in the network satisfies $\|w\|_1 \leq b$ and $|v| \leq a$. Then the class of functions $\mathcal{F} \in \mathcal{R}^{\mathcal{X}}$ defined by such a network satisfies*

$$R(\mathcal{F} \circ S) \leq \frac{1}{\sqrt{T}} \left(b^\ell + a \sum_{i=0}^{\ell-2} b^i \right).$$

We also make use of the standard lemmas; see Shalev-Shwartz and Ben-David (2014, Chap. 26).

LEMMA EC.4 (Contraction). *For each $i \in [m]$, let $\phi_i : \mathbb{R} \rightarrow \mathbb{R}$ be a ρ -Lipschitz function; namely, for all $\alpha, \beta \in \mathbb{R}$, we have $|\phi_i(\alpha) - \phi_i(\beta)| \leq \rho|\alpha - \beta|$. For $\mathbf{a} \in \mathbb{R}^m$ let $\boldsymbol{\phi}(\mathbf{a})$ denote the vector $(\phi_1(a_1), \dots, \phi_m(a_m))$. Let $\boldsymbol{\phi} \circ A = \{\boldsymbol{\phi}(\mathbf{a}) : \mathbf{a} \in A\}$. Then,*

$$R(\boldsymbol{\phi} \circ A) \leq \rho R(A).$$

LEMMA EC.5 (Convex combination). *Let A be a subset of \mathbb{R}^m and let $A' = \{\sum_{j=1}^N \alpha_j \mathbf{a}^{(j)} : N \in \mathbb{N}, \forall j, \mathbf{a}^{(j)} \in A, \alpha_j \geq 0, |\boldsymbol{\alpha}|_1 = 1\}$. Then, $R(A') = R(A)$.*

Finally, we utilize a generalization of the contraction lemma for hypothesis classes formed by vector-valued functions, established in the paper by [Maurer \(2016, Corollary 4\)](#).

LEMMA EC.6 (Vector-valued contraction). *Let \mathcal{X} be an arbitrary set, $(x_1, \dots, x_T) \in \mathcal{X}^T$, and let \mathcal{F} be a class of m -dimensional functions $f : \mathcal{X} \rightarrow \mathbb{R}^m$ and let $h : \mathbb{R}^m \rightarrow \mathbb{R}$ be an L -Lipschitz function with respect to the ℓ_2 -norm. Then,*

$$\mathbb{E} \left[\sup_{f \in \mathcal{F}} \sum_{i=1}^T \sigma_i h(f(x_i)) \right] \leq \sqrt{2}L \cdot \mathbb{E} \left[\sup_{f \in \mathcal{F}} \sum_{i=1}^T \sum_{k=1}^m \sigma_{i,d} f_k(x_i) \right],$$

where $\{\sigma_i\}_{i \in [T]}$ and $\{\sigma_{i,d}\}_{i \in [T], d \in [m]}$ are i.i.d. Rademacher random variables.

Now, we observe that the collection of vectors $\ell \circ \mathcal{H}_{\text{RUMnet}} \circ S$ is generated by composing the following operations:

1. The assortment data is the input to the RUMnet architecture that returns the utility of each choice alternative $\psi_1 : (\mathbf{z}, S) \mapsto (N_\theta(\mathbf{x}, N_{\gamma_{k_1}}(\mathbf{x}), z, N_{\eta_{k_2}}(z)))_{(k_1, k_2) \in [K]^2, \mathbf{x} \in S}$. By invoking [Lemma EC.3](#), we obtain

$$R(\psi_1(\mathbf{z}, S)) = O\left(\frac{1}{\sqrt{T}} \cdot M^\ell\right).$$

2. Next, following step 1, we apply a softmax transformation $\psi_2(\cdot)$ to the utilities of each sample of coordinate $(k_1, k_2) \in [K]^2$ of $\psi_1(\mathbf{z}, S)$. By noting that the softmax function $\mathbf{u} \in \mathbb{R}^\kappa \mapsto \left(\frac{e^{u_i}}{\sum_{j \in [\kappa]} e^{u_j}}\right)_{i \in [\kappa]}$ is 1-Lipschitz, we infer from [Theorem EC.6](#) that

$$R((\psi_2 \circ \psi_1)(\mathbf{z}, S)) \leq \sqrt{2} \cdot R(\psi_1(\mathbf{z}, S')) = O\left(\sqrt{\frac{\kappa}{T}} \cdot M^\ell\right),$$

where S' is obtained by concatenating S over the κ distinct alternatives.

3. Next, the choice probabilities outputted by the softmax operator of Step 2 are averaged over all the samples $(k_1, k_2) \in [K]^2$. This operation, represented by a mapping ψ_3 amounts to a convex combination of the output vectors, and thus, by [Theorem EC.5](#), we have

$$R((\psi_3 \circ \psi_2 \circ \psi_1)(\mathbf{z}, S)) = R(\psi_2(\mathbf{z}, S)) = O\left(\sqrt{\frac{\kappa}{T}} \cdot M^\ell\right).$$

4. Finally, the output of Step 3 is composed with the function $\psi_4 : \mathbf{p} \in (0, 1)^\kappa \mapsto \log(p_i)$ where $i \in [\kappa]$ is the index of the chosen alternative. Here, the function is $1/p_{\min}$ -Lipschitz where p_{\min} is the minimal probability attained by the RUMnet architecture. By [Claim EC.3](#) and [Lemma EC.4](#), we conclude:

$$R((\psi_4 \circ \psi_3 \circ \psi_2 \circ \psi_1)(\mathbf{z}, S)) = \frac{1}{p_{\min}} \cdot R((\psi_3 \circ \psi_2 \circ \psi_1)(\mathbf{z}, S)) = O\left(\frac{\kappa \sqrt{\kappa}}{\sqrt{T}} \cdot e^{2M} M^\ell\right).$$

CLAIM EC.3. $p_{\min} \geq \frac{1}{\kappa} \cdot e^{-2M}$.

Proof. The claim follows immediately by noting that the attractiveness of any choice alternative is lower bounded by e^{-M} and upper bounded by e^M . □

□

C.2. Proof of Proposition 4

Fix the ground truth model $\pi = \pi_N^{\text{RUMnet}}$ and $T = \lceil \frac{64}{\max\{c_1^2, c_2\} \cdot \epsilon^2} \kappa^3 e^{4M} M^{2\ell} \ln \frac{4}{\delta} \rceil$. By precisely the same line of argumentation as in Proposition 3, we have that, with probability $1 - \delta$, the following inequality holds for every $\bar{N} \in \mathcal{N}^d(K', \Theta_M^{\ell, w})$:

$$L_{\mathcal{D}}^{\text{true}}(\pi_{\bar{N}}^{\text{RUMnet}}) \leq L_S(\pi_{\bar{N}}^{\text{RUMnet}}) + c_1 \cdot \frac{\kappa\sqrt{\kappa}}{\sqrt{T}} \cdot e^{2M} M^\ell + 4c_2 \sqrt{\frac{2 \ln(4/\delta)}{T}} \leq L_S(\pi_{\bar{N}}^{\text{RUMnet}}) + \epsilon \quad (\text{EC.11})$$

By applying Hoeffding's inequality with respect to the random experiment $S \sim \mathcal{D}^T$, while using the fact that $\Pr_{s_t \sim \mathcal{D}}[|\log(\pi_N^{\text{RUMnet}}(s_t))| \leq \log(\kappa e^{2M})] = 1$ by Claim EC.3, we have:

$$\Pr_{S \sim \mathcal{D}^T} [L_S(\pi_N^{\text{RUMnet}}) - L_{\mathcal{D}}^{\text{true}}(\pi_N^{\text{RUMnet}}) > \epsilon] \leq e^{\frac{-2\epsilon^2 T}{(\log(\kappa e^{2M}))^2}}. \quad (\text{EC.12})$$

Similarly, by Hoeffding's inequality with respect to the random sampling of unobserved attributes, Claim EC.3 and the union bound, for every realization \hat{S} of S ,

$$\Pr_{N'} [L_S(\pi_{N'}^{\text{RUMnet}}) > L_S(\pi_N^{\text{RUMnet}}) + \epsilon \mid S = \hat{S}] \leq T e^{-\frac{2\epsilon^2 K'}{(\kappa e^{2wM})^2}}.$$

By plugging the definition of K' , and by taking the expectation with respect to $S \sim \mathcal{D}^T$, we obtain that

$$\Pr_{N'} [L_S(\pi_{N'}^{\text{RUMnet}}) > L_S(\pi_N^{\text{RUMnet}}) + \epsilon] \leq \delta. \quad (\text{EC.13})$$

The union bound with respect to the events of inequalities (EC.11)-(EC.13) implies that, with probability $1 - 3\delta$,

$$L_{\mathcal{D}}^{\text{true}}(\pi_{N'}^{\text{RUMnet}}) \leq L_S(\pi_{N'}^{\text{RUMnet}}) + \epsilon \leq L_S(\pi_N^{\text{RUMnet}}) + 2\epsilon \leq L_{\mathcal{D}}^{\text{true}}(\pi_N^{\text{RUMnet}}) + 3\epsilon,$$

where the first inequality proceeds from (EC.11) with the instantiation $\bar{N} = N'$, the second inequality follows from (EC.13), and the last inequality is a direct consequence of (EC.12).

By rearranging the latter inequality, we obtain:

$$\begin{aligned} 3\epsilon &\geq L_{\mathcal{D}}^{\text{true}}(\pi_{N'}^{\text{RUMnet}}) - L_{\mathcal{D}}^{\text{true}}(\pi_N^{\text{RUMnet}}) \\ &= \mathbb{E}_{(\mathbf{z}, A) \sim \mathcal{D}} \left[\sum_{\mathbf{y} \in A} \pi_N^{\text{RUMnet}}(\mathbf{y}, \mathbf{z}, A) (\log(\pi_{N'}^{\text{RUMnet}}(\mathbf{y}, \mathbf{z}, A)) - \log(\pi_N^{\text{RUMnet}}(\mathbf{y}, \mathbf{z}, A))) \right] \\ &= \mathbb{E}_{(\mathbf{z}, A) \sim \mathcal{D}} [\text{KL}(\pi_{N'}^{\text{RUMnet}}(\cdot, \mathbf{z}, A) \mid \pi_N^{\text{RUMnet}}(\cdot, \mathbf{z}, A))] . \end{aligned}$$

Table EC.1 Training parameters

Parameter	Swissmetro	Expedia	Synthetic
Activation function	ELU	ELU	ELU
Number of epochs	1,000	100	500
Early stopping	100	10	50
Regularization	None	None	None
Batch size	32	32	32
Learning rate	0.001	0.001	0.001
Tolerance	0.0001	0.0001	0.0001

Note that, in the above proof, the sampling with respect to $S \sim \mathcal{D}^T$ is unnecessary; the same line of reasoning holds by fixing any S so that (EC.11)-(EC.12) are satisfied. Nonetheless, our proof argument can be adapted to establish an algorithmic version of Proposition 4. Specifically, with respect to the hypothesis class $\mathcal{N}^d(K', \Theta_M^{\ell, w})$, the ERM estimate π_S^{ERM} on a random sample $S \sim \mathcal{D}^T$ achieves a small total learning error with high probability.

Appendix D: Additional material for Section 5

D.1. Implementation details

We use the same set of meta-parameters for all models. Since the two datasets are slightly different in size, we choose different sets of parameters for each dataset, as detailed in Table EC.1. We use the standard ADAM optimizer and the categorical cross-entropy loss function. Note that the probabilities in the cross-entropy loss are incremented by a tolerance additive factor of 0.0001 and then renormalized to avoid over-weighting small probabilities; a similar convention is utilized to compute the log-likelihood loss for all methods. Each dataset is split into a training, validation and testing sets. We also use an early stopping criterion: the gradient-descent terminates when the loss on the validation set does not improve for more than a given number of epochs. The weights from the epoch with the best validation loss are then restored. A typical profile of the loss function during the training phase is shown in Figure EC.2.

In terms of model size, Table EC.2 summarizes the number of parameters for each of the models. Note that it takes about 75 minutes on average to fit the largest RUMnet. Moderate size RUMnets can be learned much faster. For instance, for $(\ell, w) = (3, 10)$ and $K = 5$, it takes on average 14 minutes. Our main goal is to show a proof of concept and for this reason we do not attempt to optimize the hyper-parameters. There are however many practical tricks that could be used to boost the performance of neural networks, including regularization, dropout layers, scheduled learning rate, etc.

D.2. Case study: Synthetic dataset

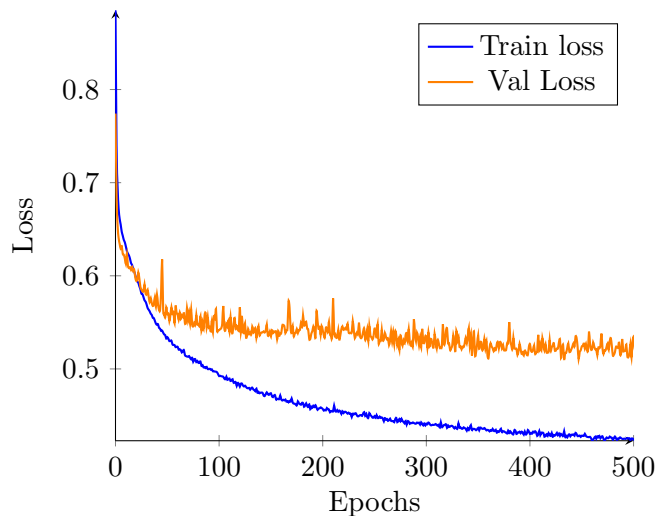
In this section, we present a case study on a synthetic dataset. The goal of this controlled experiment is to successively illustrate the benefits of RUMnets, i.e., our proposed model can capture non-

Table EC.2 Number of parameters for the different models.

Model	(ℓ, w)	K	Swissmetro	Expedia
MNL	-	-	87	92
TasteNet	(3,10)	-	1,099	1,211
	(5,20)	-	3,429	3,591
	(10,30)	-	11,019	11,201
DeepMNL	(3,10)	-	1,101	1,151
	(5,20)	-	3,441	3,541
	(10,30)	-	11,041	11,161
RUMnet	(3,10)	5	3,020	8,470
	(3,10)	10	14,500	15,520
	(5,20)	5	29,840	31,740
	(5,20)	10	55,440	58,840
VNN	(3,10)	-	1,200	14,440
	(5,20)	-	3,640	30,080
	(10,30)	-	11,340	50,820

linearity in the utility function as well as the presence of customer heterogeneity. The setup is purposely as simple as possible and, in particular, it does not include customer attributes.

D.2.1. Settings. We begin by describing three generative processes to construct synthetic datasets. For each setting, we consider a sequence of $T = 10,000$ customers, each being presented with an assortment A_t of $\kappa = 5$ products chosen uniformly at random from a universe of 50 products. Each product is endowed with a vector of attributes $\mathbf{x} = (x_1, x_2, \boldsymbol{\delta})$ where x_1 and x_2 are picked uniformly over the interval $[0, 1]$ and $\boldsymbol{\delta} \in \mathbb{R}^{50}$ is an indicator vector allowing us to introduce

**Figure EC.2** Sample loss during training phase.

fixed effects for each product. More precisely, $\delta_i = 1$ if i is the index of the chosen product and 0 otherwise. In each setting, we assume that customers choose according to a random utility model. However, the utility specification differs in each setting. We use this ground truth model to generate a choice event $\mathbf{y}_t \in A_t$, which corresponds to the product picked by the corresponding customer. Using these generated observations $S = \{(\mathbf{y}_1, A_1), \dots, (\mathbf{y}_T, A_T)\}$, we use the framework described in 4.1 to fit various RUMnet models. In particular, we experiment with $(\ell, w) \in \{(0, 0), (1, 3), (2, 5)\}$, where recall that ℓ denotes the depth of the network and w its width. For our RUMnet architecture, we also test out different number of samples $K \in \{2, 5\}$ controlling for the latent heterogeneity of customers and products. The DeepMNL model serves as a benchmark since it does not capture any latent heterogeneity (see Section 2.4). For each setting, we use 10-fold cross-validation and report the log-likelihood loss on the test set averaged over the ten splits.

Setting 1. The ground truth model is simply an MNL model. In particular, for every vector of product attributes \mathbf{x} , the utility is given by

$$U^1(\mathbf{x}) = \boldsymbol{\beta}^T \mathbf{x} + \epsilon,$$

where the entries of $\boldsymbol{\beta}$ are picked uniformly at random over the interval $[-1, 1]$ and ϵ is a standard Gumbel shock, which is sampled independently across product and customers.

Setting 2. Here, we assume that the ground truth model is described by a non-linear utility function. In particular, for every vector of product attributes \mathbf{x} , the utility is given by

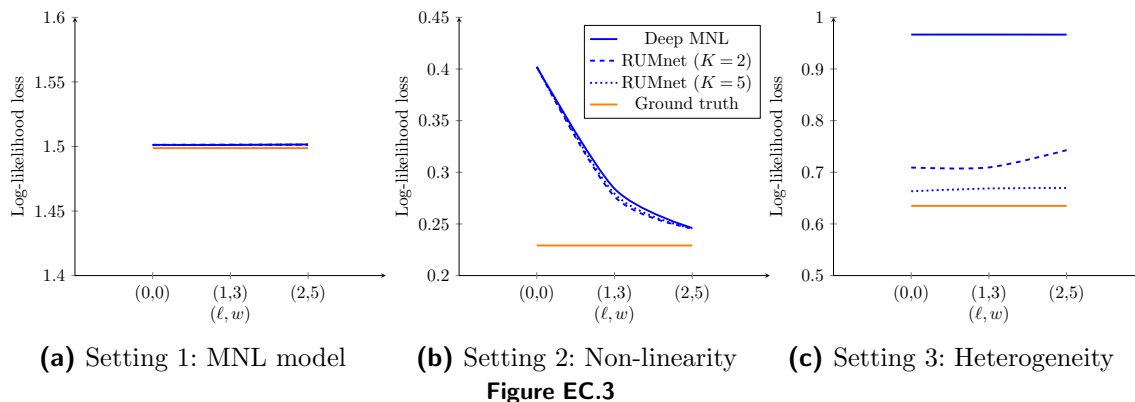
$$U^2(\mathbf{x}) = \beta_1 \cdot x_1 + \beta_2 \cdot x_2 + \beta_3 \cdot x_1^2 + \beta_4 \cdot x_1 \cdot x_2 + \beta_5 \cdot x_2^2 + \boldsymbol{\gamma}^T \boldsymbol{\delta} + \epsilon,$$

where each entry of $\boldsymbol{\beta}$ and $\boldsymbol{\gamma}$ is picked uniformly over the interval $[-1, 1]$ and ϵ is a standard Gumbel shock, which is sampled independently across products and customers. To accentuate the non-linearity effects, for this setting only, we sample x_1 and x_2 uniformly at random over the interval $[0, 10]$.

Setting 3. Our last ground truth model exhibits customer heterogeneity. Specifically, for every vector of product attributes \mathbf{x} , the utility is given by

$$U^3(\mathbf{x}) = b \cdot \boldsymbol{\beta}^T \mathbf{x} + (1 - b) \cdot \boldsymbol{\gamma}^T \mathbf{x} + \epsilon,$$

where $\boldsymbol{\beta}$ and $\boldsymbol{\gamma}$ are picked uniformly over the interval $[-100, 100]$, ϵ is a standard Gumbel shock, which is sampled independently across product and customers, and b is a Bernoulli random variable with probability of success $\Pr[b = 1] = 0.3$. Note that this model is a mixture of two MNL instances; we increase the scale of the parameters $\boldsymbol{\beta}$ and $\boldsymbol{\gamma}$ to accentuate the violation of the IIA property.



D.2.2. Results. In Setting 1, the dataset is generated using an MNL model. In this case, the utility function is linear and does not exhibit any heterogeneity. As a result, as illustrated in Figure EC.3a, the average log-likelihood loss is insensitive to the complexity of the feed-forward neural network (ℓ, w) as well as the number of samples K . In Setting 2, we construct a non-linear utility function to generate the synthetic dataset. As can be seen in Figure EC.3b, RUMnet is able to capture this non-linearity by increasing the complexity of the feed-forward neural network. In particular, as (ℓ, w) “increases”, the out-of-sample log-likelihood of RUMnet improves and it approaches that of the ground truth model, which is represented by the orange line. In this case, note that increasing K does not add much value. This is consistent with the fact that our ground truth model does not exhibit any form of customer heterogeneity. Unlike Setting 2, recall that Setting 3 has two customer classes each choosing according to a distinct MNL model. In this case, as illustrated in Figure EC.3c, the performance of RUMnet improves with K but it is mostly insensitive to the complexity (ℓ, w) of the feed-forward neural networks. Consequently, our synthetic experiments validate the value added of each component of our RUMnet architecture.

D.3. Case study 1: Swissmetro dataset

The Swissmetro is a proposed revolutionary underground system connecting major cities in Switzerland. To assess potential demand, a survey collected data from 1,192 respondents (441 rail-based travellers and 751 car users), with 9 choice events from each respondent. Each respondent was asked to choose one mode out of a set of alternatives for inter-city travel given the features of each mode such as travel time or cost. The choice set includes train, Swissmetro, and car ($\kappa = 3$). For individuals without a car, the choice set only includes train and Swissmetro. Each alternative has 4 features ($d_x = 4$) and each choice has 29 categorical features such as information about the respondent or the origin-destination pair which we transform using a simple binary encoding into a vector of size $d_z = 83$. Table EC.3 details the different features present in the data. For more information, we refer the reader to Bierlaire (2018). The original data has 10,728 observations⁵ and

⁵ <https://biogeme.epfl.ch/data.html>

Product features	Context features
Availability dummy	User group (current road or rail user)
Travel time	Travel purpose
Cost	First class traveler
Headway	Ticket type (one-way, two-way, annual pass...)
	Payer (self, employer...)
	Number of Luggage
	Age
	Income brackets
	Annual season ticket
	Travel origin
	Travel destination

has been used recurrently to test different choice modeling approach (Sifringer et al. 2020, Han et al. 2020). We preprocess the data by removing observations with unknown choice (Han et al. 2020). We retain 10,719 observations which we randomly split into training, validation and test sets with 7,505, 1,607 and 1,607 observations, respectively.

D.4. Case study 2: Expedia dataset

We next evaluate RUMnets on a dataset of hotel searches on Expedia made publicly available through the competition “Personalize Expedia Hotel Searches” hosted by ICDM in 2013⁶. Each hotel search instance $(\mathbf{x}_t, \mathbf{z}_t, A_t)$ consists of the following types of information:

- Customer attributes \mathbf{z}_t : These attributes comprise user and search query features such as the visitor’s country and search destination, the number of rooms, the duration of stay, whether there are children, how many days in advance of their trip the search is made.
- Assortment A_t : The assortment includes all hotels displayed to the user on the search result page. Each alternative has product attributes that include average user ratings, current price, average historical price, location scores, display position, among others.
- Choice $\mathbf{x}_t \in A_t$: In response to the displayed assortment, each user either booked a hotel $\mathbf{x}_t \in A_t$ or left without making any booking. As explained in the data pre-processing steps, we focus on the former type of events, meaning that we do not include the no-purchase option in the assortment.

The dataset is pre-processed as follows. For a large fraction of search queries ($\sim 30\%$), no hotel is booked. Due to this large class imbalance between the no-purchase option and specific hotel alternatives, we restrict attention to search queries that resulted in a booking. We create a one-hot encoding of the following categorical features: `site_id`, `visitor_location_country_id`, `prop_country_id`, `srch_destination_id`, whereby all categories with fewer than 1,000 occurrences are lumped into a single binary indicator. The features `price_usd` and `srch_booking_window` both

⁶ <https://www.kaggle.com/c/expedia-personalized-sort>

exhibit unrealistic values for a few choice events. We remove any search including a hotel with a negative price or a price above \$1,000. Additionally, we filter any search query made more than 1 year in advance. Consequently, we apply a log-transformation to these features. Finally, all missing observations are marked with the value ‘-1’. Following these transformations, the dataset counts 275,609 distinct search queries, 35 hotel features, and 56 customer and search features.

D.5. Additional visualizations

In Figure EC.4, we plot the choice probabilities predicted by the trained random forests as a function of the cost of the Swissmetro alternative. We observe that the variations of the choice probabilities are not monotone in contrast with RUMnets; see Figure 3 in the main paper.

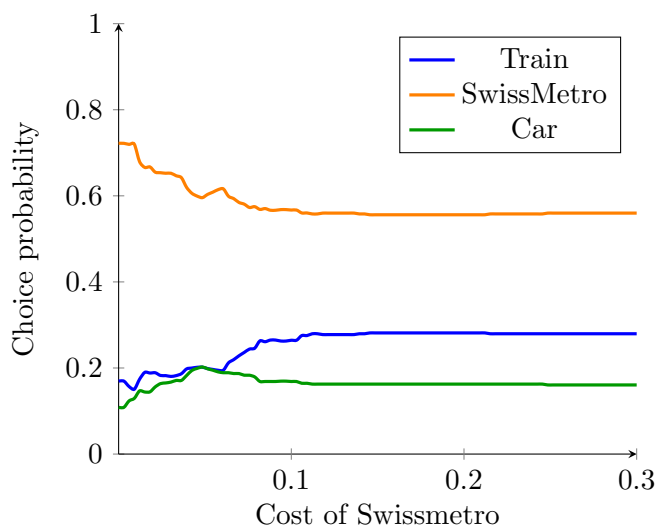
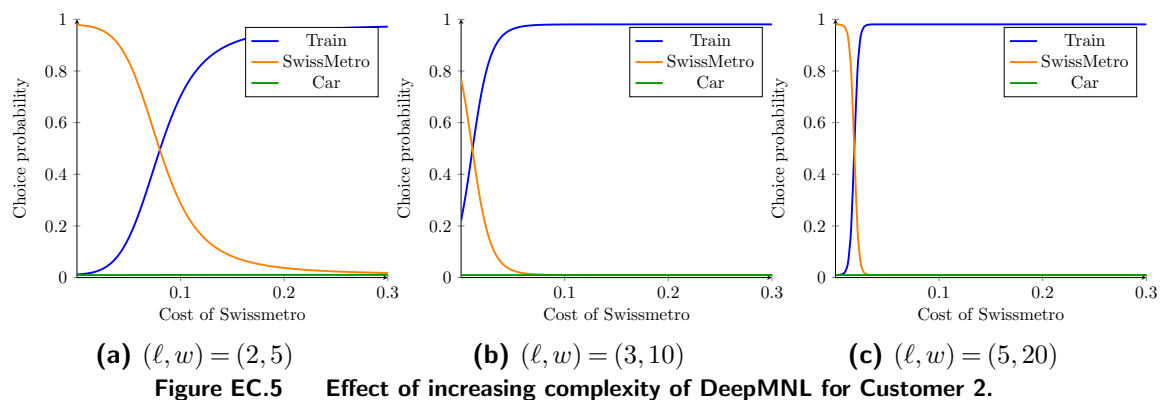


Figure EC.4 Predicted choice probabilities as a function of Swissmetro cost under the random forest approach.

Next, we explore how increasing the complexity of the RUMnet architecture affects the model structure and its resulting predictions. Two dimensions can be varied: (i) the complexity (ℓ, w) of each feed-forward neural network building block, controlling the non-linearity of the utility function, and (ii) the number of samples K , controlling the latent heterogeneity of customer and product attributes.

Figure EC.5 explores the first dimension and illustrates how the predictions of RUMnet change when the complexity of each feed-forward neural network building block is increased. In particular, Figure EC.5 shows that, for Customer 2, more complex neural networks (from left to right) capture a “sharper” substitution between Swissmetro and Train; the choice probabilities are close to either 0 or 1 and a transition occurs at the cost level that makes the customer indifferent between these alternatives. We interpret this phenomenon as follows: a more complex neural network better segments (shatters) the different types of customers, making the behavior of the resulting segments



more predictable. Figure EC.6 reveals the effect of increasing K . Latent heterogeneity implies that the choice probabilities are obtained as a mixture of different customer types. This is mirrored by the “wavelets” on the plots to the right.

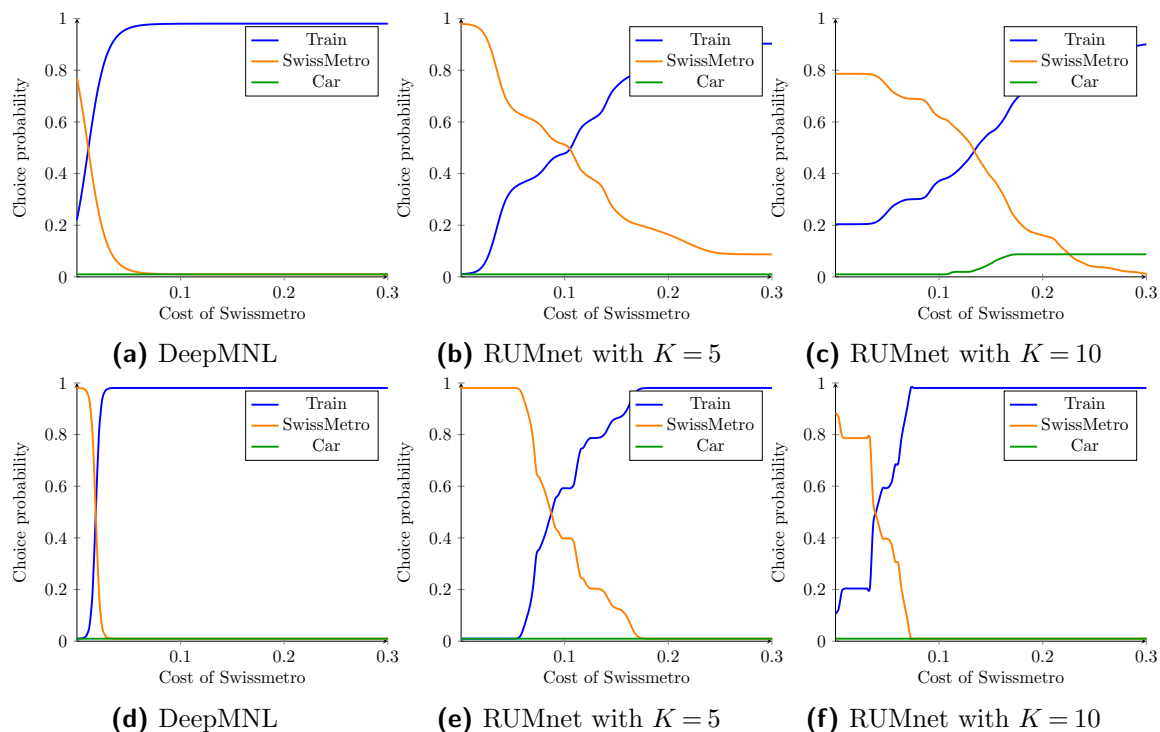


Figure EC.6 Effect of increasing heterogeneity. For all models, we have $(\ell, w) = (3, 10)$ in the first row (Figures EC.6a, EC.6b and EC.6c) and $(\ell, w) = (5, 20)$ in the second row (Figures EC.6d, EC.6e and EC.6f).

D.6. Performance of random forests on synthetic data

Although the predictive performance of the random forest (RF) approach is comparable to that of RUMnet on the Swissmetro dataset, this method has a poor performance on the Expedia dataset with a high level of overfitting (see Section 5.2). To explain this phenomenon, we hypothesize that the performance of RFs degrades as the dimension of the underlying prediction problem

increases, i.e., the number of product and customer attributes and/or the number of distinct choice alternatives which together determine the dimension of the RF inputs. In this section, we conduct synthetic experiments that support this hypothesis.

In particular, we re-use Setting 1 of our synthetic experiments, described in Section D.2. Recall that in this setting, we generate observations using an MNL ground truth model. Each customer is presented with κ products chosen uniformly at random from a universe of P products. We fix $\kappa = 5$ and experiment with $P \in \{10, 25, 50, 100\}$. Each product is endowed with a vector of attributes $\mathbf{x} = (x_1, x_2, \boldsymbol{\delta})$ where x_1 and x_2 are picked uniformly over the interval $[0, 1]$ and $\boldsymbol{\delta} \in \mathbb{R}^P$ is an indicator vector allowing us to introduce fixed effects for each product. Here, note that the input size grows with the number of products in the universe P allowing to test how the performance of the random forest scales with P . Moreover, for the random forest method, we vary the number of trees in the forest in $\{200, 300, 400\}$ and the maximum tree depth in $\{5, 10, 20\}$; we then pick the forest with the best loss on the validation set.

Figure EC.7 shows the average log-likelihood loss on the test set averaged over ten splits. We also report on this figure the average log-likelihood loss of the RUMnet model with parameters $(\ell, w) = (2, 5)$ and $K = 5$, as well as the average log-likelihood loss of a naive model, termed *RandomGuess*, that prescribes a uniform choice probability distribution over the κ offered products. We observe that as P increases, the performance of RFs diverges from that of the ground truth model and nearly matches that of *RandomGuess*. This shows that when the input dimension is large, the random forest approach is unable to learn generalizable patterns from the data. On the other hand, the predictive performance of the RUMnet model is quite insensitive to the value of P and stays relatively close to that of the ground truth model as P increases. This highlights that our method scales well with respect to the number of attributes and distinct products in the universe in contrast with model-free methods.

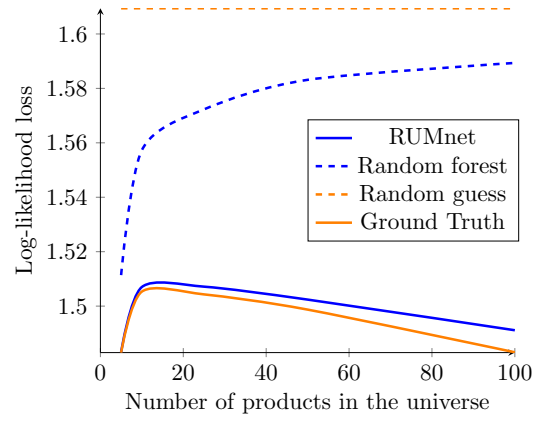


Figure EC.7 Log-likelihood loss on the test set as a function of the number of products. RUMnet has parameters $(\ell, w) = (2, 5)$ and $K = 5$.